JOURNAL OF GEOPHYSICAL RESEARCH, VOL. 87, NO. B10, PAGES 8642-8664, OCTOBER 10, 1982

# SUBDUCTION SEISMICITY AND TECTONICS IN THE LESSER ANTILLES ARC

Seth Stein, Joseph F. Engeln, and Douglas A. Wiens

Department of Geological Sciences, Northwestern University
Evanston, Illinois 60201

Kazuya Fujita

Department of Geology, Michigan State University
East Lansing, Michigan 48824

Robert C. Speed

Department of Geological Sciences, Northwestern University
Evanston, Illinois 60201

Abstract. We have studied the mechanisms of 17 earthquakes along the Lesser Antilles subduction zone to examine a site where very old lithosphere subducts at a slow convergence rate. No large thrust earthquakes occurred during the 1950-1978 study period; the three large (magnitude seven) events are all normal faults. One is a normal faulting event seaward of the trench. Its aftershock sequence includes strike slip events on differently oriented faults, probably due to lateral block motion in response to the main shock. A second indicates extension within the slab at depth. These observations suggest that subduction in this region is primarily decoupled and aseismic unless the time interval studied is unrepresentative. The third normal fault earthquake occurred within the upper plate with fault planes perpendicular to the arc and trench. This unusual geometry may represent a flexural response to the subduction of the Barracuda Ridge, a major bathymetric high with uncompensated excess mass at depth which seems analogous to flanking ridges found along some Mid-Atlantic Ridge fracture zones. Thus, the Barracuda Ridge is not buoyant and does not affect Benioff zone dip. Strike slip faulting occurs at depth in the subduction zone along a concentration normal to the arc and may indicate a fossil fracture zone. There is no direct evidence in the shallow seismicity for the hypothetical North America-South America-Caribbean triple junction though some of the oceanic 'intraplate' seismicity is consistent with such a boundary.

## Introduction

The Lesser Antilles subduction zone, along which Atlantic seafloor subducts beneath the Caribbean plate, is intriguing for both global and local tectonic reasons. It is the extreme case of the subduction of very old (∿100 m.y.) lithosphere at a very slow convergence rate (∿2 cm/yr); the nature of subduction is thus a crucial datum for 'comparative subductology.' Several major bathymetric structures are currently interacting with the trench; significant insights into the subduction of such features can be obtained. The convergence has resulted in the formation of an unusually thick and well-developed accretionary prism, which has significant effects on the subduction process. Finally, the hypothesized boundary between presumed separate North and South American plates should intersect the arc at some point; such a triple junction might be detectable in the seismicity near the boundary's intersection with the arc.

The area is shown in Figure 1 (bathymetry from Case and Holcombe [1980]). Between the Lesser Antilles volcanic arc and the Atlantic abyssal plain lie the sediments of the Tobago and Barbados troughs (forearc basins) and the Barbados Ridge complex. The Barbados Ridge is considered an accretionary prism of low-velocity, consolidated, deformed sedimentary material reaching a thickness up to 20 km and extending up to 300 km east of its crest, which includes the island of Barbados [Chase and Bunce, 1969; Bunce et al., 1970; Westbrook, 1975; Bowin, 1976; Peter and Westbrook, 1976; Biju-Duval et al., 1978; Speed, 1981a, b; Mascle et al., 1981; Moore et al., 1981]. The ridge is much wider and thicker in the southern portion of the arc. Due to the accreted sediments, no topographic trench is actually observed in the area; the ridge crest, which is marked by a Bouguer gravity minimum and lies above the shallowest Benioff zone seismicity [Tomblin, 1975], is thought to coincide roughly with the site of lithospheric subduction. The deformation front, up to several hundred kilometers seaward, marks the toe of the accretionary prism. DSDP leg 78 [Moore et al., 1981] drilled several sites near the toe and established the age of the crust (at site 543) as about 80 m.y.

South of Dominica the volcanic arc is currently active; north of Dominica the arc splits into an active western arc and an inactive eastern arc [Tomblin, 1975]. Behind the arc lies the sediment-filled Grenada Trough, considered to have been formed by back arc spreading, and the Aves Ridge, thought to be a remnant island arc [Tomblin, 1975].

Several major bathymetric highs can be observed seaward of the accretionary prism: the most noticeable are the Barracuda Ridge and Tiburon Rise, which trend northwest west of 57°W and east-west farther east. These features are



Paper number 2B0795.
0148-0227/82/002B-0795$05.00

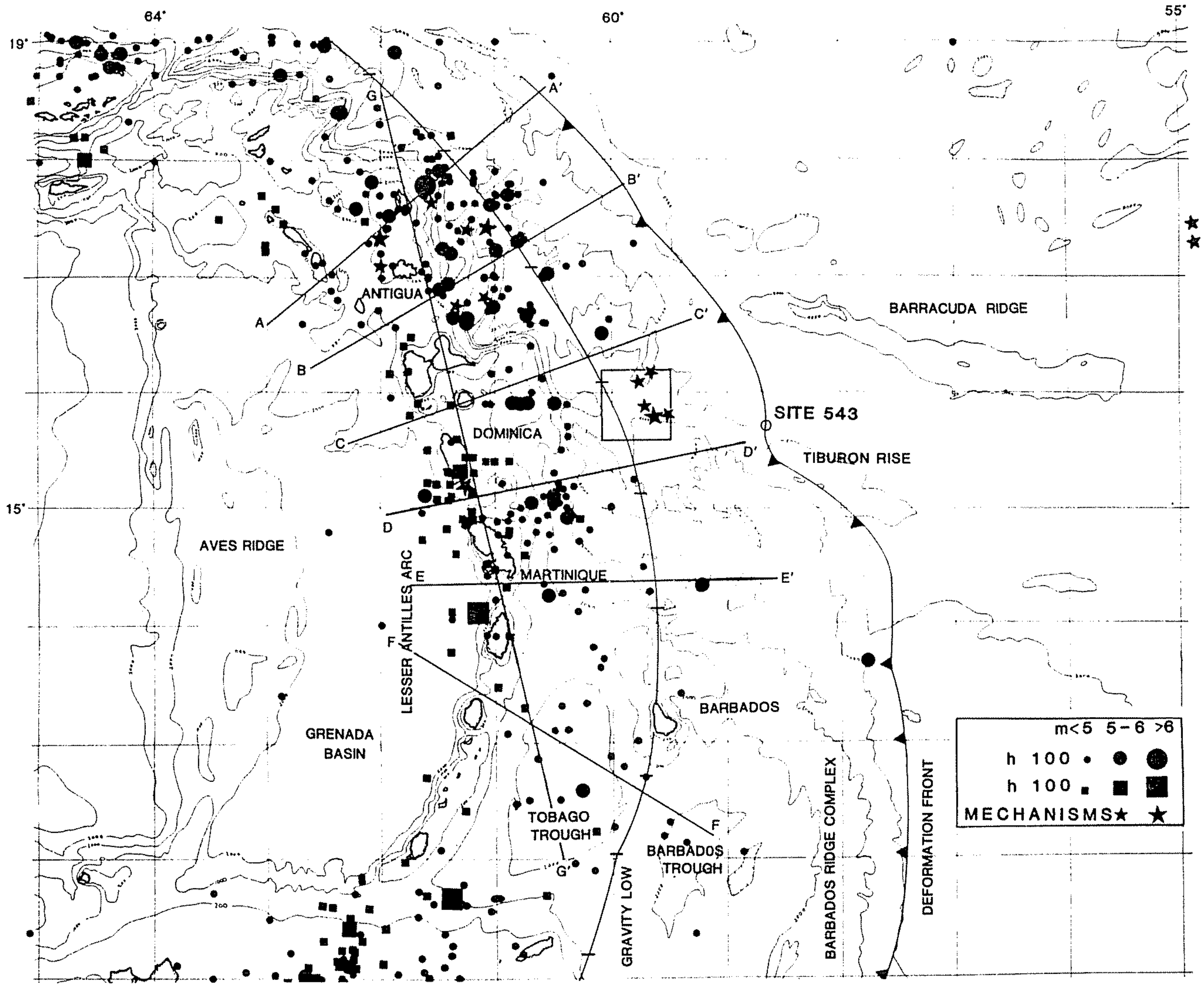


Fig. 1. Seismicity (1950-1978) of the Lesser Antilles region. Bathymetry after Case and Holcombe [1980]; 1950-1960 locations and magnitudes from Sykes and Ewing [1965]; later data from NOAA (PDE) tape. The box encloses the Christmas Day 1969 aftershock sequence; epicenters here are too dense for plotting on this scale and are shown in Figure 6. The cross sections indicated are shown in Figure 3. Stars indicate events with mechanisms from this study.

associated with major gravity anomalies [Birch, 1970; Kearey et al., 1975; Peter and Westbrook, 1976]; a buried ridge farther south (13°55'N) can be identified by a similar gravity anomaly [Westbrook, 1975]. The gravity data allow these ridges to be traced beneath the accretionary prism to the subduction zone [Keary et al., 1975; Peter and Westbrook, 1976]. The ridges affect sediment deposition and thus the shape and elevation of the accretionary prism [Westbrook, 1981].

The nature and origin of the ridges are not fully understood. The Barracuda Ridge is the best studied [Birch, 1970]. It is a high ridge with a shallow southern and steep northern slope; a sediment-filled trough lies along the north flank with a shallower trough on the south side [Birch, 1970]. Gravity and seismic refraction results [Birch, 1970] indicate thin crust and shallow mantle below the ridge. Rather than extending to the Mid-Atlantic Ridge it ends at about 55°W and shows no connection to the Researcher Ridge or Fifteen Twenty fracture zones farther east [Peter and Westbrook, 1976]. Birch [1970] proposed that the ridge was formed by uplift and normal faulting; Vierbuchen [1979] interpreted it as a scarp produced by the juxtaposition of seafloor of different ages generated by spreading in different directions. Later in this paper we propose a third model: a transform flanking ridge similar to those observed at several Atlantic fracture zones [Bonatti, 1978].

In addition to the ridges, a series of east-west trending structures can be identified in the Atlantic seafloor [Peter and Westbrook, 1976] both south of the Barracuda Ridge and in the Barbados Ridge complex. Some of these seem to show relatively recent tectonic activity; the nature of this activity and its relation to changes along the arc in the subduction process are not understood [Peter and Westbrook, 1976].

The plate tectonics of the area are understood in general but not in detail. The volcanic arc and the Benioff zone below it [Molnar and Sykes, 1969; Tomblin, 1975; Dorel, 1981] indicate the subduction of a plate, including the Atlantic seafloor below the Caribbean plate. Subduction seems to be generally perpendicular to the arc, but the direction and rate of motion are not well constrained. Figure 2 shows two successive models for plate motions in the region, computed at 15.8°N, 59.6°W (the epicenter of the Christmas Day earthquake studied here). The top result is for model RM2 [Minster and Jordan, 1978], and the lower is for the previous model RM1 [Minster et al., 1974; Jordan, 1975], showing the motions of distinct North American (NA) and South American (SA) plates with respect to the Caribbean (CA). The overall result indicates subduction at about 2 cm/yr oriented somewhat north of west. This subduction rate is in accord with the Benioff zone length predicted by thermal models [Molnar et al., 1979; Davies, 1980].

The boundary geometry of the Caribbean plate poses difficulties for relative motion determination [Jordan, 1975; Minster and Jordan, 1978]; since rate information can be obtained at only one point, the small spreading center in the Cayman Trough [Holcombe et al., 1973; Macdonald and Holcombe, 1978]. Furthermore, two major boundary segments, the Greater Antilles [Burke et al., 1978, 1980; McCann and Sykes, 1981] and the South American [Rial, 1978] suggest complex and perhaps intraplate deformation possibly distributed over a broad zone. Finally, as discussed later, it is difficult to obtain useful directional information from focal mechanisms in the Lesser Antilles, since most of the earthquakes are intraplate rather than interplate.

The major difference between RM1 and RM2 is in the relative motion between possibly distinct North and South American plates. Ladd [1976] used Atlantic magnetic anomalies to show that from 180 to 9 m.y. B.P. South America had resolvable motion with respect to North America. Global inversions of present-day relative motion data [Minster et al., 1974; Chase, 1978; Minster and Jordan, 1978] also show resolvable differences between North America-Africa and South America-Africa Euler poles, implying two distinct American plates. Alternatively, the difference may result from a microplate southeast of the Azores not included in the inversions (N. Sleep, personal communication, 1982).

There is no clear evidence for a North America-South America plate boundary, either in bathymetry or seismicity; thus both its location and sense of motion are unknown. In the absence of direct measurements, relative motion has been estimated from differences in the Euler vectors. The resulting motion is quite slow and poorly constrained since the NA-SA difference is small and the pole lies close to the Caribbean. Small changes in relative motion models thus produce quite different NA-SA motions. This motion has been drawn in Figure 2, for illustrative purposes, as a pure transform motion. Ball and Harrison [1970] and Minster and Jordan [1978] suggest that since the motion may be distributed over a broad zone between 10° and 20°N and may be largely aseismic, definition of this boundary may not be possible.

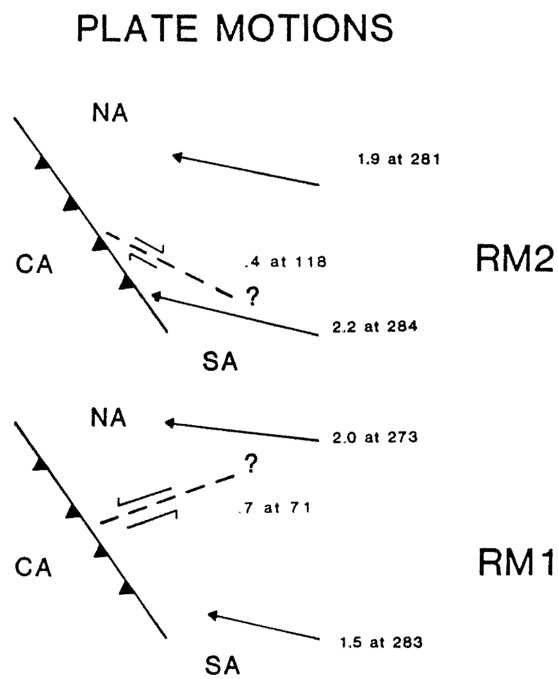


Fig. 2. Relative plate motions at 15.8°N, 59.6°W showing North (NA) and South (SA) American plates with respect to Caribbean (CA). The overall convergence rate and azimuth do not depend seriously on the relative motion model used; the proposed NA-SA motion is shown as pure transform and depends more on the model. RM1 is from Minster et al. [1974] and Jordan [1975]; RM2 is the more recent version [Minster and Jordan, 1978].

The boundary (or boundary zone) may intersect the arc, possibly at about 15°N, where the level of seismicity changes and the Benioff zone is deepest [Peter and Westbrook, 1976; Vierbuchen, 1979]. Alternatively, Bowin [1975] suggested that the Barracuda Ridge may mark part of the boundary, which would then not intersect the arc. The other end of the hypothetical boundary, at the Mid-Atlantic Ridge, has been studied by Vierbuchen [1979], who suggested a change in transform orientation, and Le Douaran and Francheteau [1981], who identified a depth anomaly. Thus at both ends it seems plausible, but not established, that either a diffuse or discrete boundary exists.

We searched for possible focal mechanisms at the arc end of the boundary; none were identified. Since the North America-South America question is unresolved, it is unclear whether the subducting plate should be regarded as 'North America,' 'South America,' or both. In the absence of better information we treat the subducting plate as a single plate, thus assuming that any relative motion is small compared to the convergence rate.

## Seismicity

The seismicity of the area has been studied by Sykes and Ewing [1965], Molnar and Sykes [1969], Tomblin [1975], and Dorel [1981]. Figure 1 shows epicenters from the NOAA (PDE) tape covering the period 1961-1978 and from Sykes and Ewing [1965] for 1950-1960. Epicenters

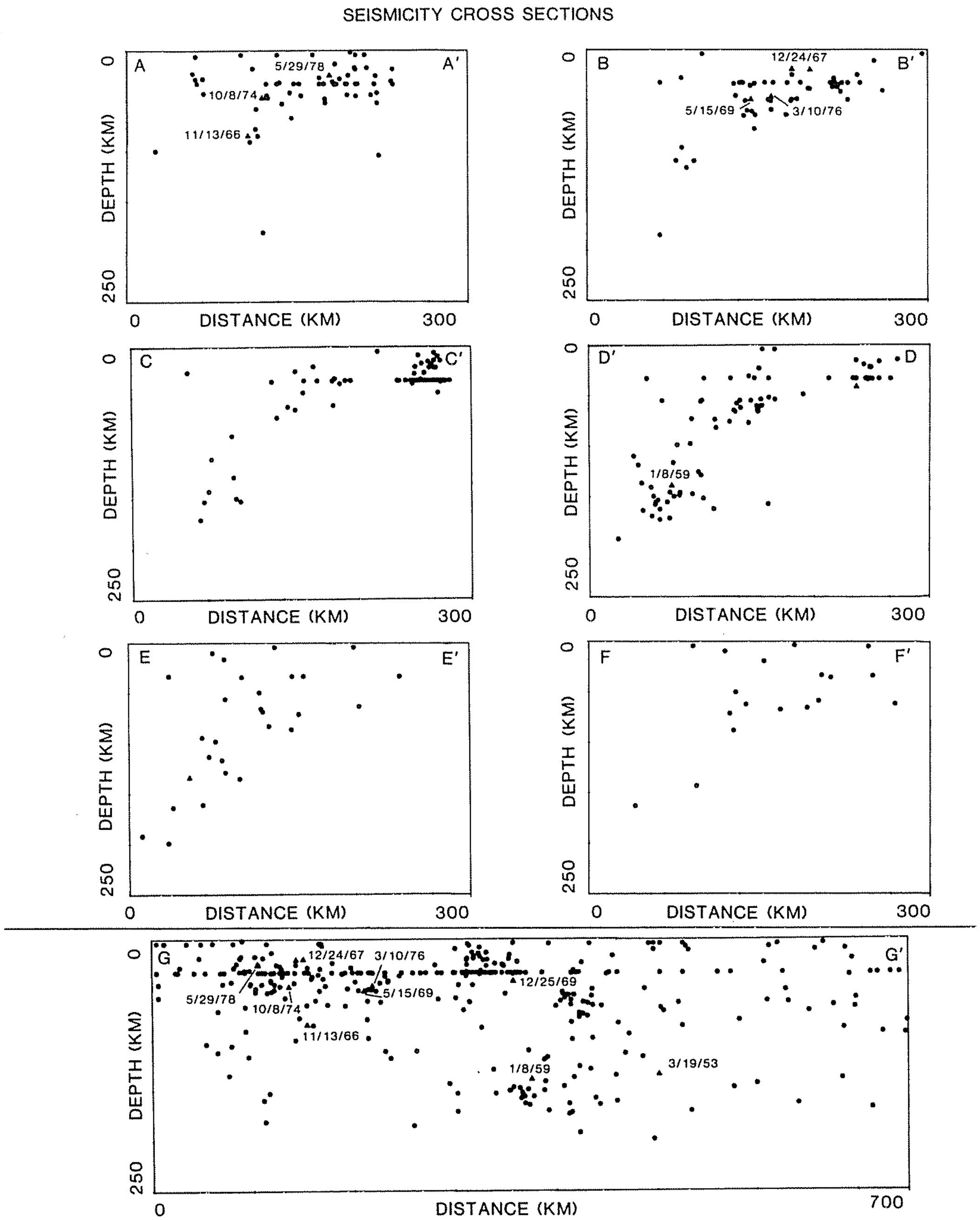


Fig. 3. Seismicity cross sections for the profiles shown in Figure 1. AA'-FF' are perpendicular to the arc; GG' is parallel to the arc. The depths are from the epicenter tape except for events studied here, labeled with dates, for which our preferred depths were used. Changes in dip and activity level are noticeable along the arc. The northern section (AA'-BB') is the most active and has shallow events; the center (CC'-DD') is less active and deeper; the south (EE' and FF') is the least active. (Section GG' shows a 33-km artifact due to the tape's default depth.)

have been sorted by body wave magnitude and depth with the attendant uncertainties. The box at about 59.9°W, 16°N indicates the aftershock zone of the 1969 Christmas Day (Ms 7.5) earthquake; the epicenters are too dense to plot on this scale and are shown in detail in Figure 6. Stars indicate events for which we have obtained focal mechanisms. We focus our attention in this paper on the arc itself, north of about 12°N.

The first obvious observation is that the seismicity level is rather low for a subduction zone. Only five large ($m_b$>6) events occurred in the arc itself in the 28-year period, presumably due to the slow subduction rate and the weak coupling of the plates, as discussed later.

Most of the seismicity occurs arcward of the gravity low, which is assumed to mark the subduction trace. The Christmas Day 1969 sequence, as discussed later, is a noteworthy exception.

TABLE 1. Events Studied

| Date | Location (ISC) | | Mechanism | | | m | Ms | Mo, dyne cm | Depth | |
|---|---|---|---|---|---|---|---|---|---|---|
| | Lat. °N | Lon. °W | $\phi$ | $\delta$ | $\lambda$ | | | | ISC | This Study |
| March 19, 1953 | 14.1 | 61.21 | normal fault unconstrained | | | | 7.5 | | | 135 (S) |
| January 8, 1959 | 15.25 | 61.26 | 292 | 74 | 355 | | 6.5 | | | 141 (S) |
| October 23, 1964 | 19.8 | 56.11 | 302 | 62 | 160 | 6.2 | 6.8 | $4.5 \times 10^{25}$ | 43 | 30 (L) |
| November 13, 1966 | 17.05 | 61.94 | 320 | 83 | 270 | 5.4 | | | 92 | 73 (P) |
| December 24, 1967 (2003) | 17.42 | 61.19 | 141 | 84 | 310 | 6.1 | 6.3 | $5.4 \times 10^{25}$ | 42 | 15 (L) |
| December 24, 1967 (2132) | 17.61 | 61.26 | 306 | 87 | 53 | 5.9 | | | 5±10 | 17 (P) |
| May 15, 1969 | 16.75 | 61.39 | 348 | 72 | 112 | 5.7 | 6.0 | $1.1 \times 10^{25}$ | 50 | 50 (L) |
| December 25, 1969 (2132) | 15.79 | 59.64 | 168 | 74 | 255 | 6.4 | 7.5 | $7.8 \times 10^{26}$ | 1±12 | 42 (R) |
| December 25, 1969 (2231) | 16.08 | 59.79 | 200 | 82 | 4 | 5.8 | | | 6±12 | 37(R);47(P) |
| December 26, 1969 | 15.79 | 59.56 | 300 | 70 | 185 | 5.3 | | | 12 | 38(R);35(P) |
| December 29, 1969 | 16.18 | 59.74 | 180 | 64 | 270 | 5.5 | 5.9 | $9.7 \times 10^{24}$ | 33 | 39(R);27(P) |
| January 7, 1970 | 15.86 | 59.78 | 310 | 80 | 50 | 5.5 | 6.2 | $1.3 \times 10^{25}$ | 37 | 41(R);40(L);35(P) |
| October 8, 1974 | 17.37 | 61.99 | 250 | 58 | 270 | 6.4 | 7.4 | $2.5 \times 10^{26}$ | 41 | |
| March 10, 1976 | 16.84 | 61.06 | 255 | 82 | 130 | 5.7 | 6.2 | $2.6 \times 10^{25}$ | 56 | 56 (P) |
| December 13, 1977 | 17.33 | 54.91 | 244 | 68 | 65 | 5.7 | 6.9 | $5.4 \times 10^{25}$ | 51 | 25 (L) |
| May 29, 1978 | 17.17 | 61.59 | 184 | 66 | 329 | 5.2 | 5.4 | $5.0 \times 10^{24}$ | 48 | 25 (P) |
| December 6, 1978 | 17.44 | 54.83 | 233 | 69 | 45 | 5.4 | | | | |

Depth abbreviations: S, Sykes and Ewing [1969]; L, long-period body wave modeling; P, short-period depth phase; R, relocation.

A few small events may be within the accretion prism itself, though this may be a mislocation effect. The Christmas Day sequence is below the prism in the underlying lithosphere. Chen et al. [1982] suggest that no events occur within the prism near Barbados and that accretionary prisms are, in general, aseismic.

Figure 3 shows seismicity cross sections along the profiles in Figure 1: six perpendicular to the arc and one along it. (The latter clearly shows the 33-km artifact of the default depth.) Triangles indicate the events studied here and thus the largest events. For these events, as discussed in the following section, we were often able to determine depths and plot events more accurately than using the depth given by the PDE.

A major difference in seismicity, noted by Tomblin [1975] and Dorel [1981], occurs between the northern (north of 14°N) and southern portions of the arc. The southern region is substantially less active than the northern one. Dorel [1981] shows that historical seismicity follows a similar pattern. Tomblin [1975] and Dorel [1981] also noted that the deepest seismicity is concentrated in the area just south of Dominica (15.2°N) with a possible E-W trend; we will show that strike slip faulting occurs at depth here. Dorel [1981] suggested that the Benioff zone dip is steepest in this area and shallows to the north and south. (In the southern segment the dip is more difficult to define because of the low seismicity.) There are thus three regions: an active, shallow, northern region; an active, steeper, central region; and a less active, southern region. These differences could be a sampling time effect due to the low seismicity level or, if real, may result from a plate boundary [Vierbuchen, 1979], the effect of bathymetric ridge subduction, or the accretionary prism.

The present data set is not adequate to indicate or exclude the possibility of a double seismic zone [Hasegawa et al., 1978; Fujita and Kanamori, 1981; Seno and Pongsawat, 1981]; Dorel's [1981] study using local seismic net data also did not indicate a double zone.

## Focal Mechanisms

We studied the mechanisms of 17 events in the Lesser Antilles and the nearby seafloor. These can be divided into three groups: a main shock-aftershock sequence associated with normal faulting just seaward of the trench, the arc seismicity, and 'intraplate' events well seaward of the subduction zone. In this section the mechanisms and depths are discussed; tectonic implications are treated in the following section. The results are listed in Table 1.

Several of these events have been previously studied by other investigators [Molnar and Sykes, 1969; Rial, 1978; Dorel, 1978; Liu and Kanamori, 1980; Dewey et al., 1980; Bergman and Solomon, 1980; McCann et al., 1982]. In addition, several events not discussed here have been previously studied. These studies are listed in the appendix and Figure A1, which cover both the arc region studied here and an area to the south.

### Christmas Day 1969 Sequence

The largest earthquake we studied was the main shock of a major sequence that occurred in

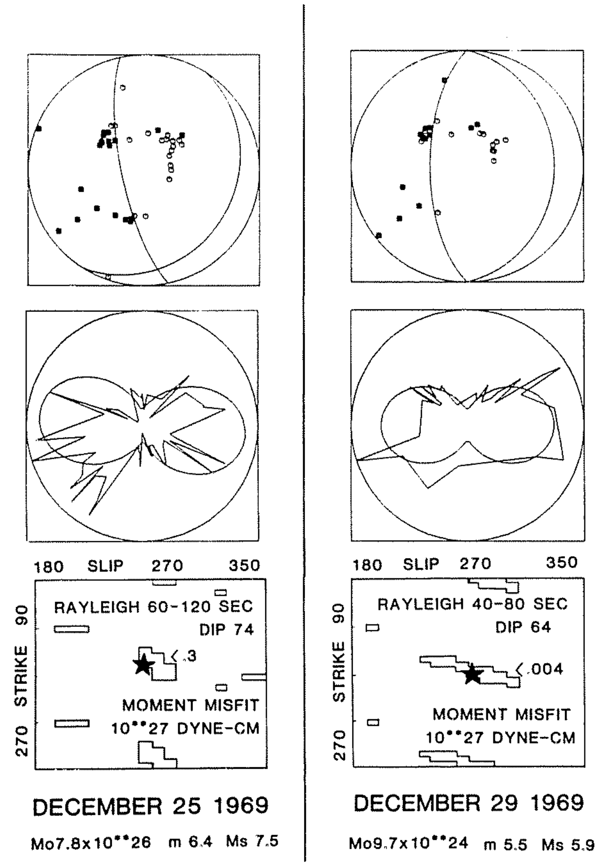


Fig. 4. First motion data (lower focal hemisphere, solid symbols compressional), theoretical and observed Rayleigh wave amplitude radiation patterns, and misfit contour plots for the Christmas Day main shock and a large aftershock with a similar mechanism.

late December 1969 and early January 1970. These events are unusual in their location well seaward of the gravity low and the other seismicity (Figures 1 and 3).

Figure 4 (left) shows the results for the main shock of the sequence on Christmas Day 1969. The first motions (upper left) from WWSSN records show almost pure normal faulting with a well-constrained N-S trending plane dipping steeply west. The second nodal plane is constrained by a single clear close-in first motion at TRN to have some strike slip component. The solution shown is a best fit to the amplitude radiation pattern of Rayleigh waves, using both R1 and R2, equalized to 90°. The velocities for the equalization were from earth model 5.08 M [Kanamori, 1970]; Q values are from Tsai and Aki [1969].

The data (middle left) show a clear two-lobed radiation pattern suggestive of primarily dip slip faulting. For the dip angle constrained by the first motion data, theoretical amplitude radiation patterns were computed for fault strikes ranging from 0° to 360° and slip angles from 180° to 360° (which are equivalent to those for slip 0°-180°). The best fitting seismic moment, using the L1 or median norm, and the associated errors were calculated for each strike and slip pair; for noise-free data the correct mechanism would yield the exact moment at each station. The L1 norm was chosen due to its robust properties in handling noisy data [Claerbout, 1976]. The lower left portion of Figure 4 shows a contour plot of the results. The minimum misfit (best fit) regions are clearly concentrated; the star shows our preferred mechanism, the best fit consistent with the first motions for which the theoretical radiation pattern (left center) was computed. (Such plots vary only slowly with dip; if a wide range of dips were acceptable, a series of plots was made.) For the strike and dip of the N-S plane, the first motions allow slips from about 235° (roughly equal strike slip and normal faulting) to about 255° (almost pure normal faulting). Increasing slip angles result in lower misfit, which can be seen as a clockwise rotation of the theoretical lobe pattern. Thus a slip of 270°, pure normal faulting, provides a slightly better fit but violates the one first motion point at TRN, which may be affected by the slab. Naturally, for tectonic interpretation the two mechanisms are indistinguishable. The seismic moment and surface wave magnitudes we obtained, along with the ISC body wave magnitude, are shown on the figure.

We used this general approach of combining the first motion and surface wave data for most of the earthquakes studied; the presentation will be the same as in Figure 4. We attempted to satisfy both types of data whenever possible. Both have problems. Ray paths in an island arc region can be significantly distorted by the presence of the cold, high-velocity slab [Sleep, 1973; Fujita et al., 1981]. It is thus reasonable to suspect nearby stations and those along the strike of the arc of mislocation on the focal sphere. In some cases, like this earthquake, the surface wave data would be better fit by discarding some body wave data. The surface wave data are prone to other difficulties. In addition to true noise, considerable attenuation [Rial, 1976] inhomogeneities in the arc region and global path effects produce apparent 'noise.' The equalized spectral amplitudes were averaged over several period windows, and the one yielding the smoothest result was used. The robust properties of the L1 norm usually were adequate to provide good constraints from the surface wave data, which appear as concentrated regions in the strike versus slip contour plots. In some cases, usually corresponding to badly scattered data, the good fit regions were fairly broad and thus provide weaker constraints. When possible, body wave modeling was also used. Since a common solution was sought for first motion, surface wave, and body wave data, the approach implicitly does not allow for different body and surface wave mechanisms.

Figure 4 (right) shows the results for one of the largest aftershocks in the sequence, the December 29, 1969, event. Both body and surface wave data are fit well by pure dip slip faulting on a N-S plane. Small strike slip components are not preferred by the data but are acceptable. This solution is quite similar to the main shock.

Figure 5 (left) shows a slightly bigger aftershock, on January 7, 1970. One nodal plane, striking NW-SE, is well constrained; the second cannot be drawn to satisfy all the close-in (SJG, TRN) and along strike (BEC) first motions. The surface wave and body wave data gave the preferred solution shown, which misfits first motions at only one of these three stations. A pure dip slip solution would misfit all three. Figure 5 (right) contains mechanisms for two other aftershocks. The only data available are short-period first motions; the December 26, 1969, event is small, and the December 25, 1969, one occurs within an hour of the main shock, so both long-period first motions and surface waves are obscured. The short-period first motions are often ambiguous and scatter somewhat but imply similar strike slip faulting for both earthquakes. ISC bulletin reported first motions (not shown) show the same pattern with similar scatter. The dashed lines (Figure 5) show nodal planes consistent with the data but subject to reasonable uncertainty.

We also explored the spatial relationships of the aftershock sequence. The epicenter tape locations show a general N-S trend to the aftershock zone, but the depth of faulting is unclear. In particular, the ISC gives the depth of the main shock as 1±12 km. The depth of faulting for this sequence bears significantly on its tectonic interpretation.

The main shock and the two large (January 7, 1970; December 29, 1969) aftershocks were relocated using arrival times from the ISC bulletin:

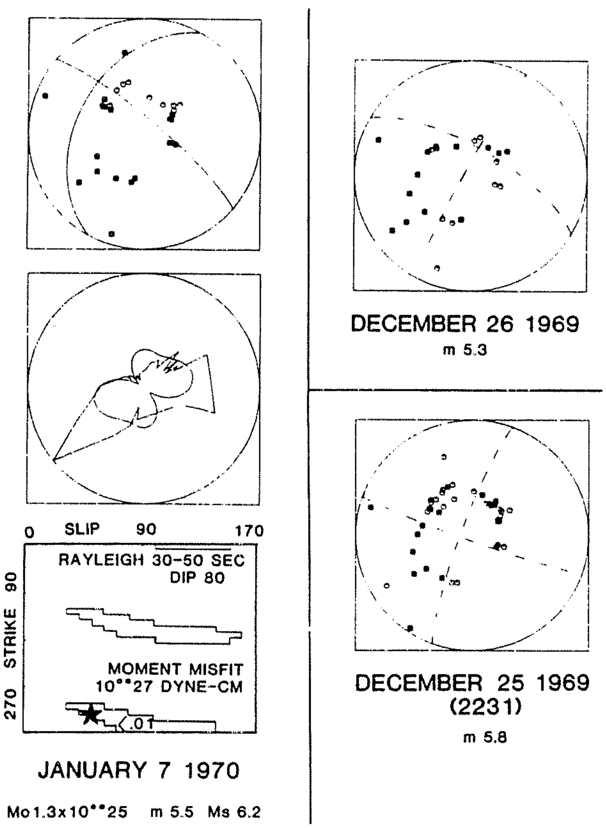


Fig. 5. First motion and surface wave data for the January 7, 1970, aftershock (left); short-period first motions for two other aftershocks (right). All three events have significant strike slip components and are quite different from the main shock and December 26, 1969, aftershock. Weakly constrained nodal planes are dashed.

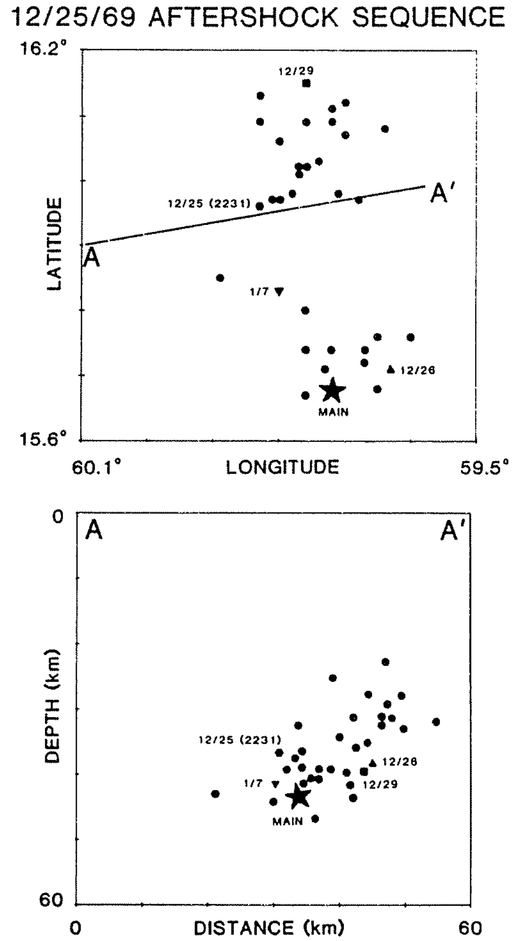


Fig. 6. Christmas Day aftershock sequence relocated relative to January 7, 1970, aftershock. The map view (top) indicates a N-S fault plane; the depth section (bottom) indicates a west dipping fault plane.

The January 7, 1970, event gave the smallest residuals at a depth of 41 km. As this agreed with body wave modeling results (discussed next), it was used as a master event. Figure 6 shows the results of relocating the 35 largest events (each with 40 or more reported arrivals) relative to the January 7, 1970, event, using the Jeffreys-Bullen travel time table. The epicenters (top) are aligned approximately N15°W, with a suggestion of northern and southern clusters. The hypocenters (bottom), projected on the AA' cross section, show a trend dipping about 55° to the west. All aftershocks locate deeper than 22 km; the shallowest of the five large events is at 37 km. This geometry suggests that the west dipping N15°W nodal plane is, in fact, the fault plane.

A second method of depth determination is to use the body waves. Unfortunately, crustal structure in the focal region is not well known; the major uncertainty is in the thickness of the low-velocity accretionary prism. Multichannel seismic data about 75 km south of the area [Mascle et al., 1981] show at least 4 s (two way) of sediment; the thickness is known to vary considerably within the prism. Since depth deter-

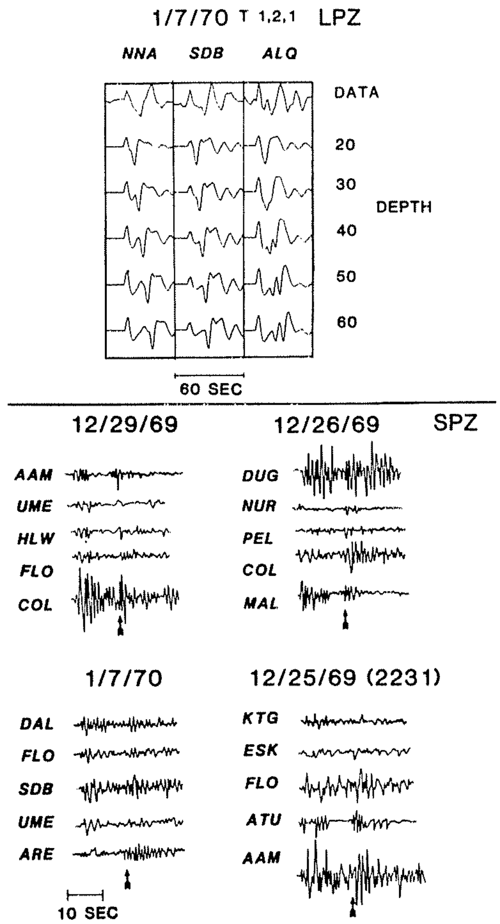


Fig. 7. Long-period (top) and short-period (bottom) P waves for events in the Christmas Day aftershock sequence. Only January 7, 1970, had modelable long-period P waves; the focal depth appears to be 40±5 km. Arrows indicate the short-period depth phase interpreted as pwP on the short-period records.

minations rely on observed travel times and assumed velocities, uncertainties in structure produce depth uncertainties.

Figure 7 (top) shows long-period vertical P waves at three WWSSN stations for the January 7, 1970, event. Synthetic body waves were calculated using the standard shallow earthquake modeling technique [Langston and Helmberger, 1975; Kanamori and Stewart, 1976; Helmberger and Burdick, 1979; Stein and Kroeger, 1980], a model with a water layer over a solid half space, the focal mechanism from Figure 4, and a 1,2,1 trapezoidal time function. A 7-km/s half-space velocity was used to stimulate the effects of a 6-km-thick layer of 4-km/s sediment, a 7-km-thick crust with velocity 6.8 km/s, and an 8.1-km/s mantle. The data show the effects of water reverbations, which are well fit at these stations, and near-source (or receiver) structure, which the model does not include. The best fits are for a depth of about 40±5 km.

The short-period vertical records of the same event (Figure 7, bottom) show a clear depth phase about 14 s after the P wave. Modeling studies of Aleutian earthquakes [Hong and Fujita, 1981] suggest that this arrival may be pwP, the reflection from the sea surface, which is usually more prominent on short-period than long-period records and is a valuable depth indicator [Forsyth, 1982]. The assumption that the depth phase is pwP can be used [Stein, 1978] to reconcile short-period depth phases with long-period body wave modeling results. Assuming the phase to be pwP yields a depth of 35±5 km; for this depth, pwP is reinforced by sP, which arrives at a similar time. Thus, the relocation, long-period, and short-period body waves agree to their accuracy on a depth of about 40 km.

Short-period depth phases for the other events (Figure 7, bottom) also indicate depths in the 30 to 50-km range; these events do not have modelable long-period P waves. The relative depths agree in general but not completely with those in Figure 6. Without a crustal structure accurate enough for detailed short-period modeling, it is not clear whether the difference results from variations in structure between events spread over 60 km or from the 'depth phase' being more complicated than a single pwP arrival, especially since the mechanisms of the four events differ.

The body wave and depth phase data thus support the relocation results of 30 to 50-km depths for the aftershock sequence and provide credibility to the 42-km depth given by the relocation for the main shock. The aftershock zone can be used to estimate the fault area. For a 25 km (width) by 50 km (length) fault area, a moment of $7.8 \times 10^{26}$ dyne cm and a rigidity of $5 \times 10^{11}$, the average slip would be about 1.2 m. The long dip slip fault stress drop relation [Starr, 1928; Kanamori and Anderson, 1975] yields 21 bars, with the usual large error bounds [Stein and Kroeger, 1980]. These values agree reasonably well with the scaling relations and tabular data of Geller [1976]; in fact, the fault width chosen is half the length, the approximation used there for $M_s$ versus fault area relations. The tectonic implications of the sequence are discussed in a later section.

## Island Arc Focal Mechanisms

We studied nine earthquakes in the arc region itself, using the techniques previously discussed. Five events were large enough for surface wave study; body waves were modeled for three and short-period depth phases were examined for five. Two occurred prior to the availability of WWSSN data so International Seismological Summary reports were used for first motions. In this section we briefly discuss the data for each event.

The largest is the October 8, 1974, earthquake located 41 km below the arc itself, north of Antigua. First motion and surface wave data (Figure 8, left) require primarily normal faulting on a NE-SW plane. The formal best fit to the scattered surface wave data is pure normal faulting; a component of strike slip motion on the SE dipping plane as proposed by McCann et al. [1982] based on aftershock relocations is also quite acceptable. This mechanism is interesting since the faulting is clearly not parallel to the arc, as often observed.

The next largest pair of events (Figure 8, right, and Figure 9) are slightly seaward of the arc on December 24, 1967: one at 2003 hours and a smaller one at 2132. First motion data for the first event (Figure 8, right) constrain a NW-SE nodal plane. The surface waves favor a mixed strike slip and dip slip solution but can accommodate slip either near 315° or 225°. These correspond to a second plane striking as shown in the figure but dipping either NW or SE. The solution shown provides a somewhat better fit to the body waves (Figure 9, top) than the alternative. The mechanism shown for the second shock (lower right, Figure 9) is from short-period records, since the long periods were swamped by the earlier event. The dashed nodal planes shown are consistent with the data and similar to the first shock.

The depths of these events show whether they are in the subducting plate or the overriding plate. The ISC depths for the two are 42 and 5±10 km, respectively. Body wave modeling, with a water layer over a half space of velocity 6.2 km/s suitable for the island arc [Boynton et al., 1979], favors a depth of about 15 km for the first event (Figure 9, top), shallower than given by the ISC. Short-period records (Figure 9, lower left) of the second event show a possible depth phase of about 9 s after P. Treating this as pwP yields a depth of about 17 km which agrees well with the first event, and implies

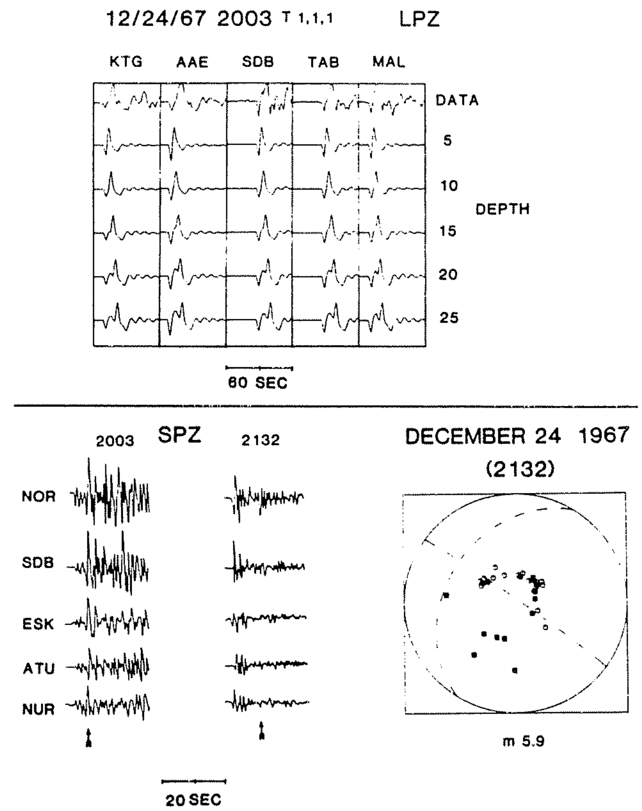


Fig. 9. (top) Body wave modeling results for the first event of December 24, 1967, indicating a focal depth of about 15 km rather than the ISC's 42 km. (lower left) The first event consists of a small foreshock followed by the main event (arrow). The second event shows a possible depth phase (arrow), which yields a pwP depth about 17 km, similar to the first event. (bottom right) Short-period first motions for the second event, 1½ hours later, are consistent with a mechanism similar to the first.

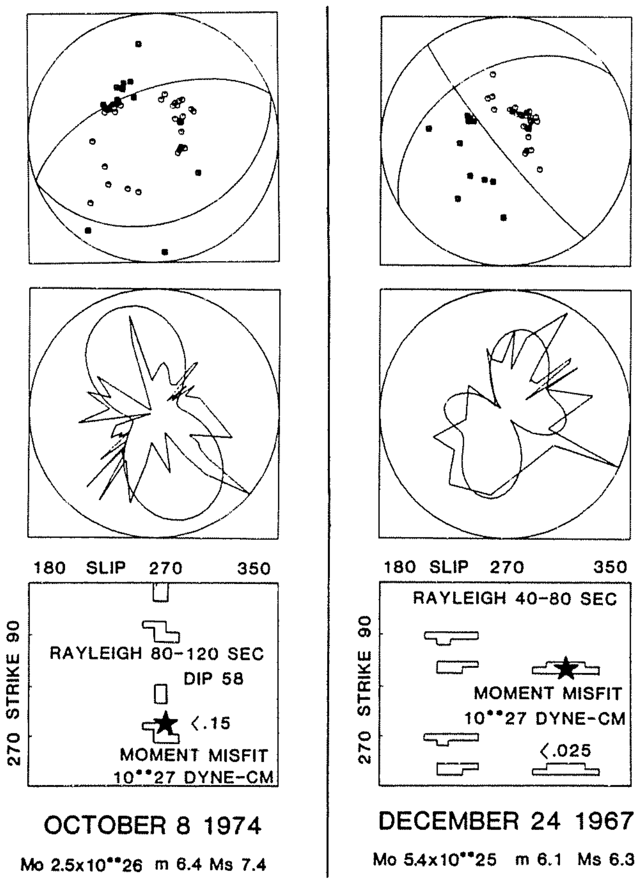


Fig. 8. First motion and surface wave data for the large normal faulting earthquake near Antigua (left) and for the first of two events on December 24, 1967 (right). The Rayleigh waves for the October 8, 1974, event include both R1 and R2 equalized to 90°.

that both occur within the overriding plate. Short-period records of the first event (Figure 9, lower left) show the presence of a small foreshock 3 s before the event; this also appears on the long-period records at KTG, MAL, and TAB (Figure 9, top) as a slow drift preceding the main arrival and may have contributed to the ISC's depth overestimate.

The March 10, 1976, event occurred to the south of the December 24, 1967, pair, in a similar location near the steep slope seaward of the arc. First motion data (Figure 10, left) constrain a NE-SW nodal plane; the surface waves indicate mixed strike and dip slip faulting. This solution shown (slip 130°) is consistent with the first motions; the alternative (slip 60°-80°) is less so. The depth given by the ISC (56 km) agrees with a short-period depth phase about 20 s after the P wave, if treated as pwP, and with long-period body wave modeling.

The next event studied occurred on May 15, 1969, about 40 km arcward of the March 10, 1976, event. First motions indicate nearly pure thrust faulting (Figure 11); the surface wave data are poor. The solution chosen does not fit the surface wave data well but fits the first motions

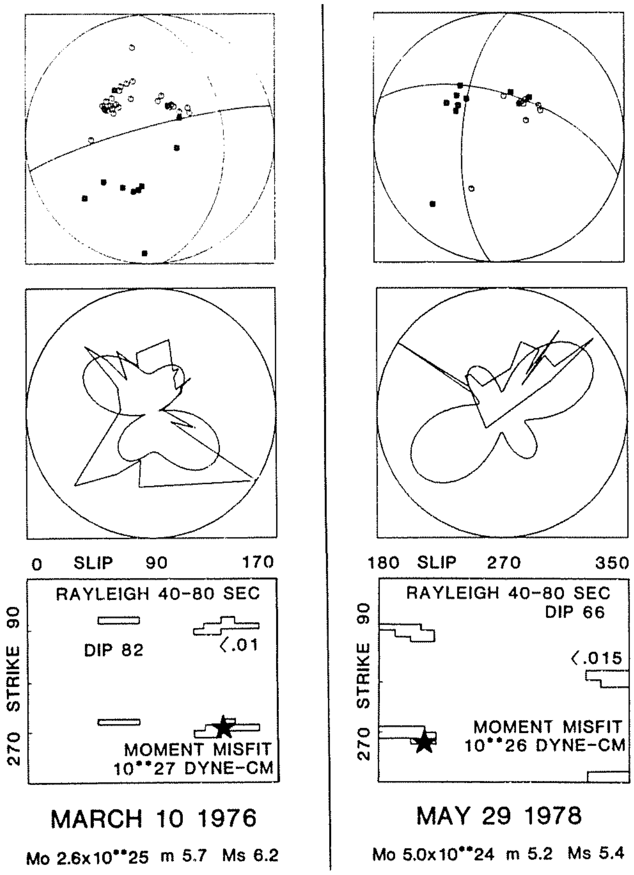


Fig. 10. First motion and surface wave data for the March 10, 1976, earthquake (left) and the May 29, 1978, earthquake (right). The May 29, 1978, event is the smallest event for which surface wave data was usable, thus the results have considerable uncertainty.

and good long-period body waves (Figure 11, bottom). The best fitting depth is about 40 km, somewhat shallower than the ISC depth of 50 km.

Only one other event yielded usable surface waves--the May 29, 1978, one shown in Figure 10, right. Both first motions and surface waves are small and at the lower limit of our analysis methods. The solution shown agrees with both data sets but is still subject to uncertainty. The ISC gives a depth of 49 km; depth phases about 9 s after P imply a slightly shallower 35-km depth.

All the events discussed so far are comparatively shallow: above 60 km. Few deeper events large enough for study occurred since 1963; none yield unambiguous mechanisms. One small deeper event (m 5.4) on November 13, 1966, yielded short-period first motions (Figure 11, left center) consistent with pure dip slip faulting on either a near vertical or shallow dipping plane striking NW-SE, although a strike slip solution is also acceptable. Depth phase arrivals about 20 s after P yield a 73-km depth; the ISC gives 92 km. We also examined International Seismological Summary (ISS) reports of the deepest large earthquakes in the arc prior to the availability of WWSSN data. One, on January 8, 1959, at a depth of 141 km [Sykes and Ewing, 1965], can be interpreted as strike slip faulting (Figure 11). The other, on March 19, 1953, at a depth of 135 km [Sykes and Ewing, 1965], is clearly primarily normal faulting but with unconstrained nodal planes (Figure 11). The other large events prior to 1963 did not have enough reported first motions to make such analysis meaningful.

## Atlantic 'Intraplate' Events

Three events in the Atlantic seafloor well seaward of the trench were also studied. The first, on October 23, 1964, occurred well to the east of the northernmost protion of the arc. The first motions (Figure 12) indicate a NW-SE nodal plane and place little constraint on the second. The body wave data are quite good and provide tighter constraints than the surface waves. Figure 13 (center) shows that the best slip angle

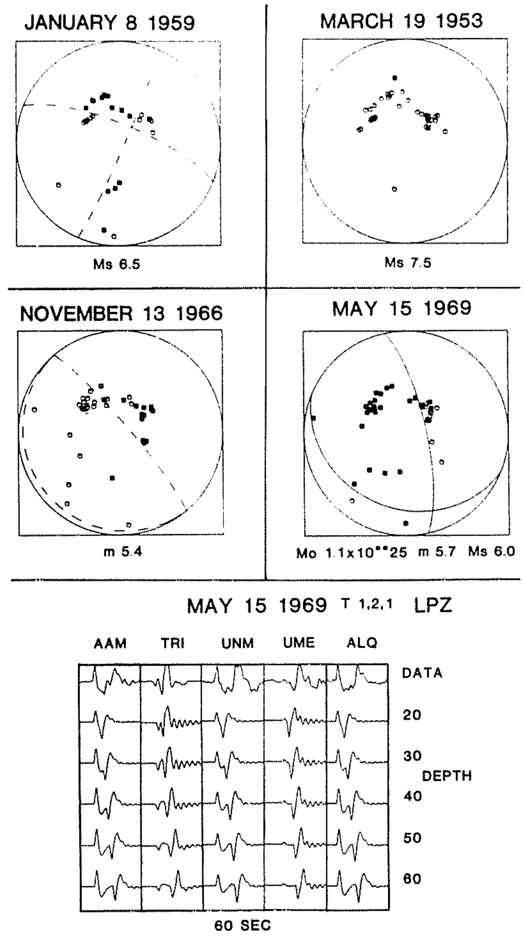


Fig. 11. (upper left) ISS first motions suggesting strike slip faulting for an event 141 km deep in the active seismic zone below Dominica. (upper right) ISS first motions for a large event at a depth of 135 km which suggests almost pure normal faulting; nodal planes are unconstrained. (middle left) Short-period first motions suggesting dip slip faulting in the downgoing slab. (middle right) First motions and surface wave data for the May 15, 1969, event. (bottom) Body wave modeling results implying a depth about 40 km. This is the only event studied that suggests thrusting at the plate boundary.

on the NW-SE nodal plane is slightly greater than 160°, that the strike of the nodal plane is very near 300° (top left), and that the focal depth is about 30 km (top right). Surface wave data for this event are poor but consistent with the indicated result. This mechanism is similar to that of Molnar and Sykes [1969] and Liu and Kanamori [1980].

Two interesting intraplate events occurred in December 1977 and 1978 north of the Barracuda fracture zone. The first was studied using first motion, surface wave data (Figure 12, left) and body wave modeling (Figure 13, bottom). This solution agrees with that of Bergman and Solomon [1980]. The second, much smaller, yields only short-period first motions. The first event exhibits well-constrained thrust faulting with some strike slip component; the second is much less constrained but can be interpreted as very similar to the first. The body waves yield a focal depth of 25 km, shallower than the unusual ISC depth of 51 km.

## Tectonic Implications

### Lithospheric Normal Faulting

The Christmas Day sequence shows normal faulting on a plane steeply dipping toward and parallel to the arc. It is located well seaward of what would be the 'trench' in the absence of sediments and occurs at shallow (less than 50 km) depth. The large moment and spatial extent of this earthquake sequence suggest that it is one of the major normal faulting events within the subducting lithosphere which are currently a topic of considerable interest. The type examples include the 1933 Sanriku [Kanamori, 1971, 1977], 1965 Rat Island [Stauder, 1968; Abe, 1972], and 1977 Indonesian [Stewart, 1978] events.

The aftershock distribution (Figure 6) strongly implies that the N15°W striking, west dipping nodal plane of the main shock was the fault plane. The main shock, both in the ISC and the relocation results, occurred at the south end of the aftershock zone, implying a northward unilateral rupture. The relocation suggests that the main shock occurred at the deepest point of the aftershock zone; if correct, implying unilateral updip rupture. The complex character of the long-period body wave suggests the rupture occurred as a series of smaller 'point source' events.

The four aftershock mechanisms (Figure 14) provide some ideas about stress release in the two weeks following the main shock. The December 29 event is the most similar to the main shock and suggests further normal faulting on the main fault plane or one parallel to it. The others are more curious in that they have major (January 7) or dominantly (December 25 and 26) strike slip motion, with nodal planes significantly different from the main shock and December 29 event.

Figure 15 (top) shows compressional (P) and dilatational (T) axes from the focal mechanisms. Clearly, all five earthquakes do not have similar axes, though the main December 25, 26, and 29 events have similar near horizontal T axes. One possible interpretation is that the T axis of the main shock gives the extensional deviatoric

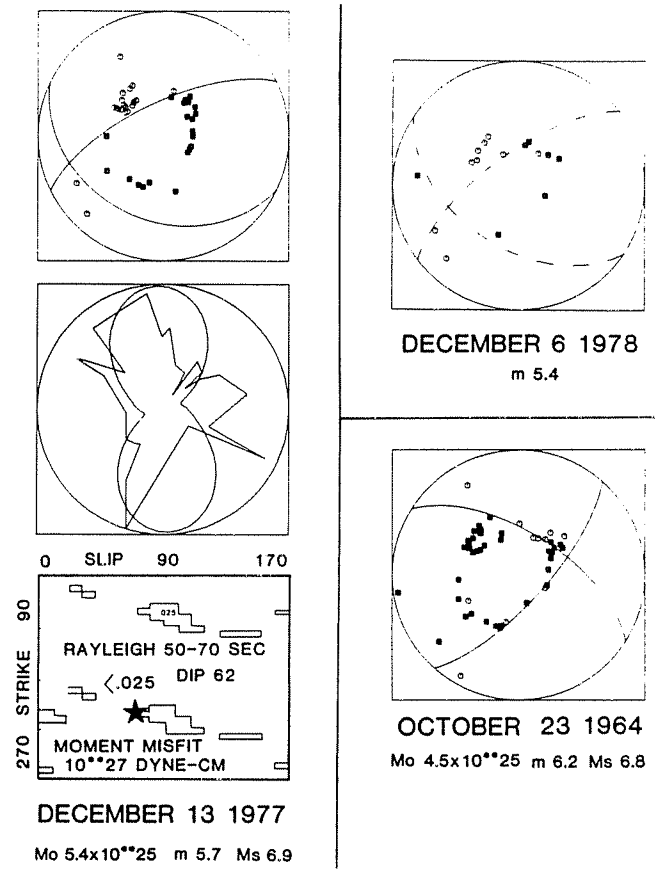


Fig. 12. (left) First motion and surface wave data for a large event well seaward of the trench. (top right) Short-period first motions for a smaller event in the same place 1 year later, consistent with a similar fault geometry. (bottom right) First motions for another large Atlantic event. Body wave data (see Figure 13) were also used to constrain the solution shown.

stress direction, since the main shock results from a new fracture formed in the lithosphere. The smaller aftershocks occur on preexisting weak zones, so their P and T axes have only weak relations to the overall stress field [McKenzie, 1969; Stein, 1979].

A more useful criterion may be the orientation of the horizontal components of the slip vectors (Figure 15, top); the arrow gives hanging wall motion with respect to the footwall. Some ambiguity results since two possible fault planes exist, each with a corresponding slip direction. Solid arrows indicate one possible choice for each event; dashed arrows indicate the other. Only one direction is shown for the main shock, since the west dipping plane is assumed, and for the December 29 aftershock, since the two horizontal slip directions are antiparallel. The NW-SE planes for the three partially strike slip aftershocks give horizontal slip directions consistent with the main shock and normal fault aftershock.

We suggest that the aftershock sequence, including the many events too small for mechanism study, consisted of a response to the large extensional faulting main shock composed of two types of motion shown schematically in Figure 16.

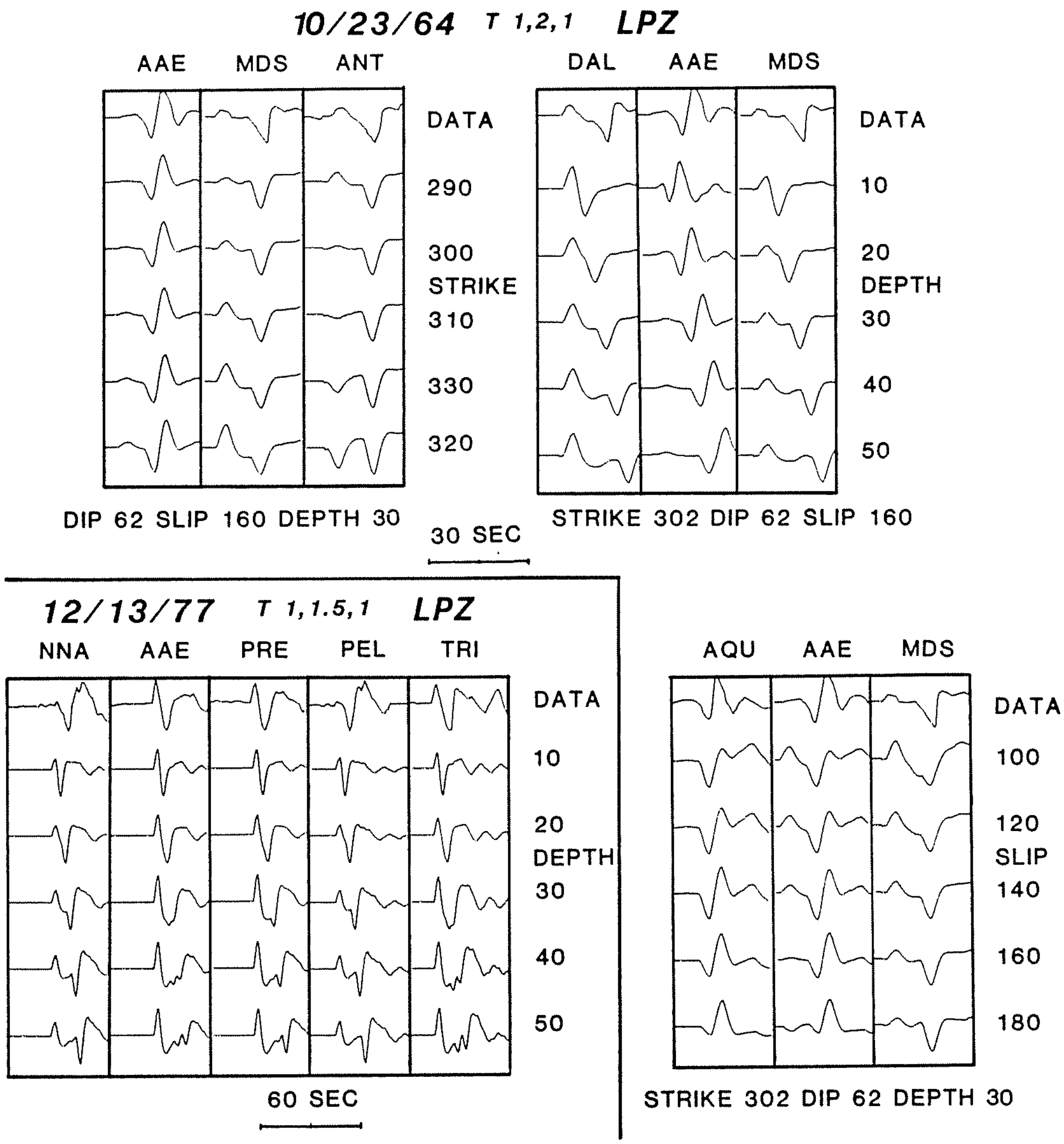


Fig. 13. Body wave modeling results for the two large Atlantic events. (top) October 23, 1964, indicating the mechanism shown in Figure 12 and depth of about 30 km. (bottom) December 13, 1977, indicating a depth of about 25 km, in contrast to ISC's 51 km.

One, shown by the December 29 event, is further normal faulting, on the original fault plane or a nearly parallel plane. The second is horizontal block motion on preexisting fractures near the main fault plane. The subducting plate contains many smaller fractures as well as the major NW-SE structures like the Barracuda Ridge and Tiburon Rise [Peter and Westbrook, 1976]. Blocks bounded by such faults may have moved to accommodate the displacement produced by the main shock. Note that in this geometry, block motion can yield opposite senses of strike slip on parallel planes. The block motion could occur either arcward or seaward of the main fault; the locations do not exclude either possibility. Some NW-SE fractures in the subducting plate seem to have had comparatively recent motion [Peter and Westbrook, 1976]; one possible source of such motion is this block faulting.

Strike slip block faulting is not always observed after such large lithospheric normal faulting events; none was noted by Fitch et al. [1981] for the 1977 Indonesian event. Possibly the geometry of that earthquake was atypical due to its location near the collision of Australia with the arc [Fitch et al., 1981; Cardwell et al., 1981], or no fractures of the appropriate orientation occurred near the epicenter.

Two general models have been offered for large lithospheric normal faulting events. Kanamori [1971, 1977] and Uyeda and Kanamori [1979] interpret these earthquakes as failure of the subducting lithosphere due to the weight of the downgoing slab. In this model, such earthquakes indicate that the subducting plate is partially decoupled from the overriding plate and that subduction may be at least partially aseismic. The alternative view, due to Chapple and Forsyth [1979], views these large normal fault earthquakes as simply the largest examples of normal

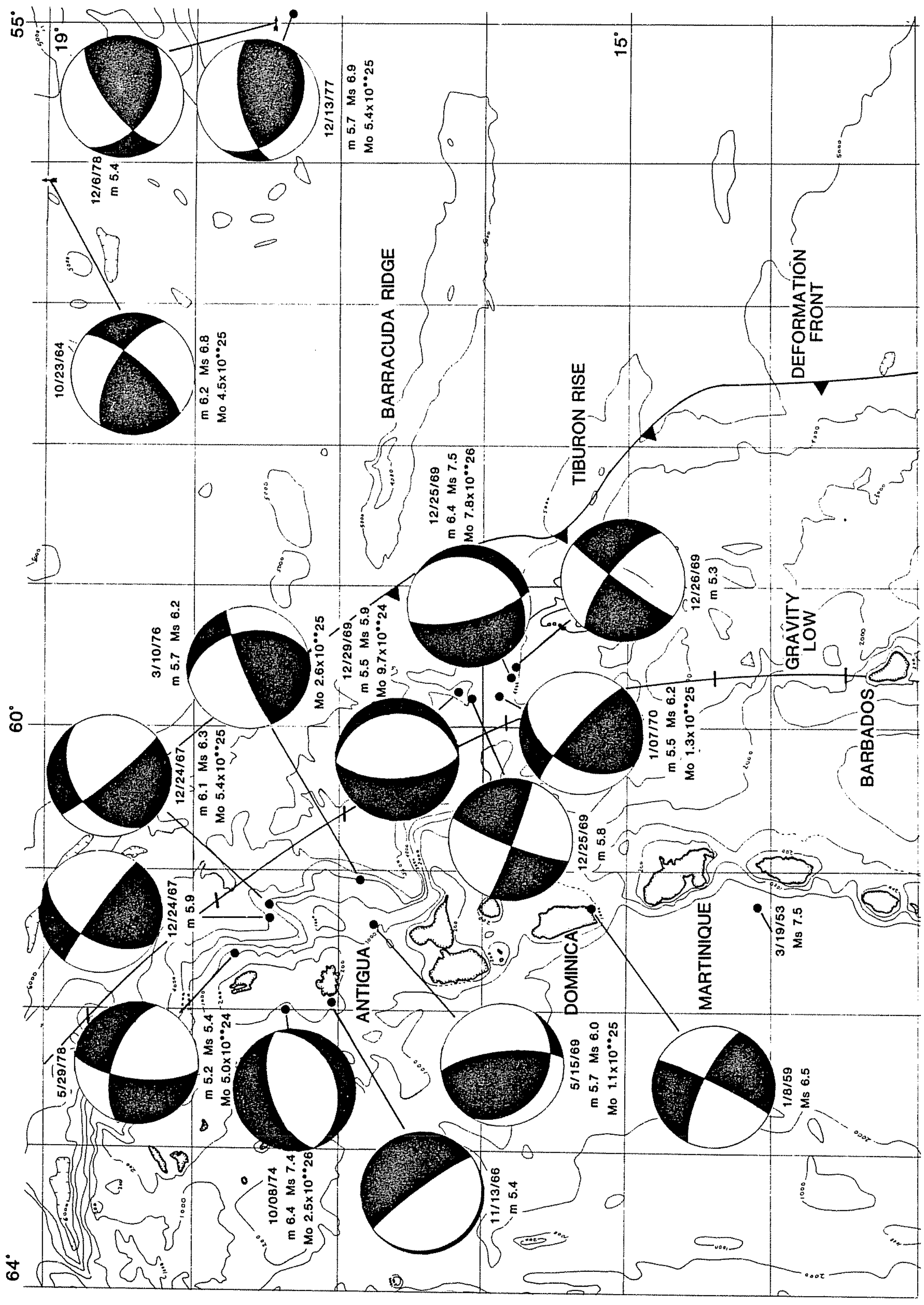


Fig. 14. Focal mechanism results for this study. Two events (October 23, 1964; December 8, 1978) are slightly off the map.

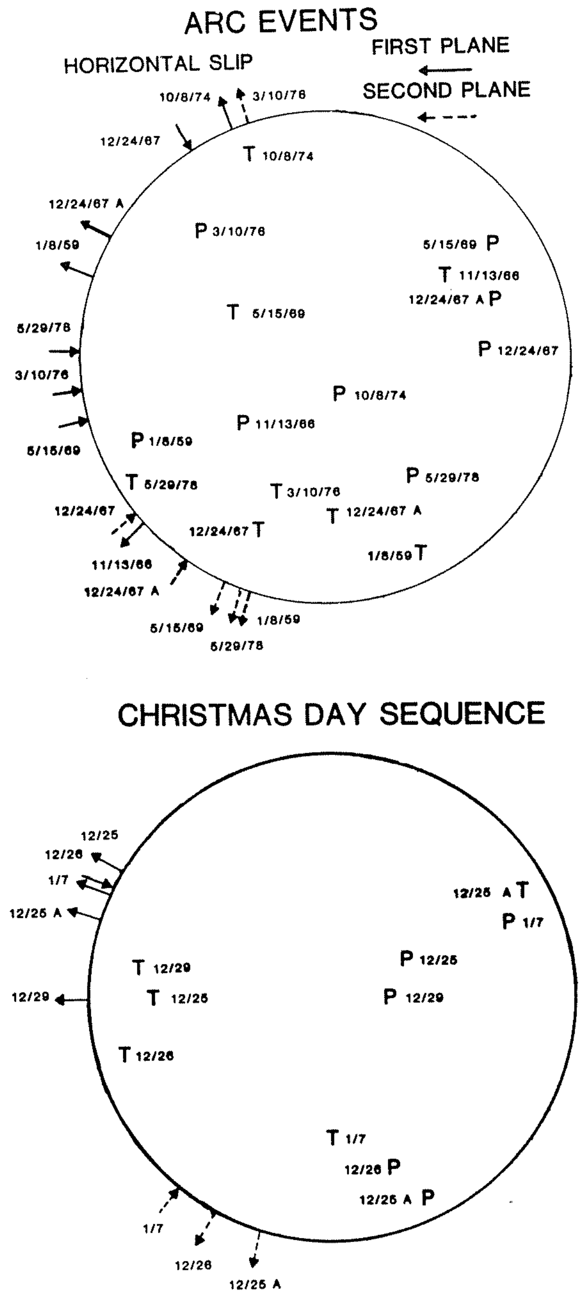


Figure 15. (top) Horizontal slip vector components and P and T axes for the Christmas Day sequence. West dipping nodal planes were used for the main and December 29 events; both choices are shown for the other strike slip events. For the NW-SE planes, the horizontal slip directions are similar to those for the two normal events. (bottom) Horizontal slip directions and P and T axes for all island arc events.

faulting events due to flexure of the downgoing lithosphere seaward of the trench [Chen and Forsyth, 1978; Frolich et al., 1980]. Both models are consistent with the mechanism observed; as discussed later, Dorel [1981] has proposed from a moment release argument that subduction here may be partially aseismic.

The maximum depth of faulting provides one possible discriminant between the two models; faulting to the base of the lithosphere (70 km) supports the Kanamori [1971, 1977] model. On the other hand, faulting to a shallower depth can be ascribed either to a failure of the lithosphere under its weight which tears only partially through the lithosphere or to failure in extension above the flexural neutral sheet. Our analysis of the aftershock sequence indicates that faulting did not extend deeper than 50 km. Assuming that the accretionary wedge is at least 7 km thick, the maximum depth of faulting is less than 45 km within the oceanic lithosphere. The 1965 Rat Island normal faulting earthquake [Abe, 1972] also appears to have faulted only partially through the lithosphere. This does not necessarily exclude the Kanamori [1971, 1977] model if the lower portion of the lithosphere undergoes either delayed seismic faulting or aseismic slip to complete the tearing process. The relative depths of the main shock and aftershock sequence may provide another constraint; flexure-generated faulting might be more prone to begin near the top of the lithosphere where the greatest extensional fiber stress occurs rather than at depths approaching the neutral sheet in the middle of the lithosphere where flexural stress is a minimum. The flexure and decoupling models are not mutually exclusive; both effects acting together would depress the position of the neutral plane. Better depth data would be one way to investigate these questions.

The minimum depth of faulting, based on the relocation of the largest aftershocks, seems to be about 20 km, implying that faulting did not involve the accretionary prism. This is consistent with studies which have found no seismicity within prisms [Chen et al., 1982] and implies low rigidity for even the deeper, more consolidated portions of the prism.

An interesting question is whether any information about plate motion directions can be drawn from the faulting geometry since the faulting is purely within the oceanic plate rather than on the interplate boundary. The horizontal slip direction is more northerly than would be expected for the convergence (Figure 15). The fault strike, N15$^{o}$W, is roughly both parallel to the island arc and perpendicular to the convergence. One way to interpret the geometry is to examine the 1965 Rat Island normal fault earthquake [Abe, 1972], since at this location, subduction is highly oblique. There the fault strike was parallel to the subduction zone rather than perpendicular to the convergence direction, and the horizontal slip aligns with neither. Using this analogy, we can derive little relative motion information from the Christmas Day results.

## Arc Earthquakes

The focal mechanisms in the arc region (Figure 14) seem unusual for a subduction zone. Only one moderate size event (May 15, 1969) shows thrust faulting in a geometry suggesting slip at the plate boundary. (Dorel [1978] shows several other small thrust events, as listed in the appendix.) The other earthquakes are dominantly strike slip or normal faulting. Seismicity cross sections, on the other hand, show a clear Benioff zone (Figure 3). In this section we attempt to

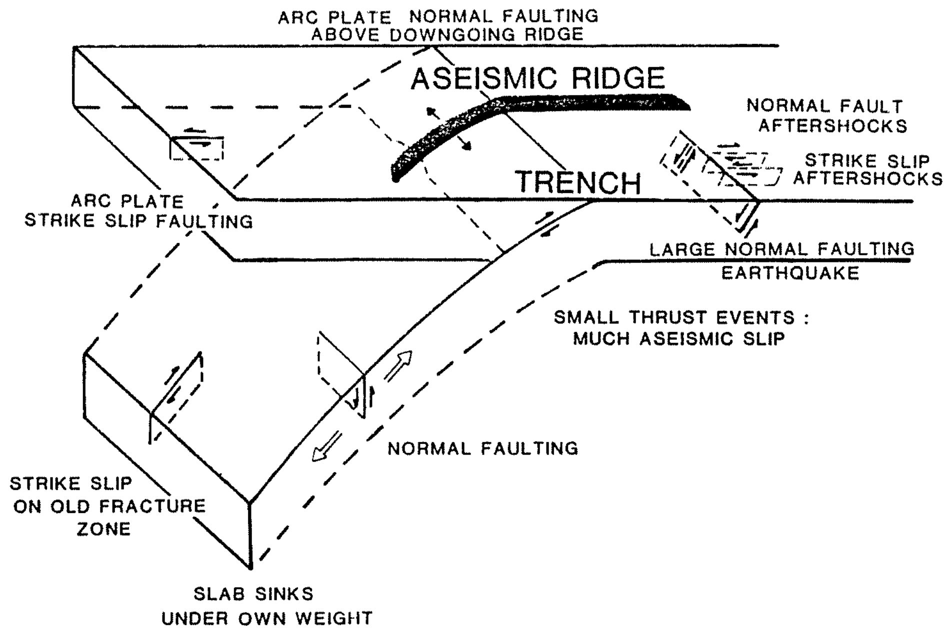


Fig. 16. Schematic tectonics of the study area. For simplicity, the accretionary prism is not shown, and both subduction and weak zones are drawn perpendicular to the trench.

provide tectonic interpretations for the unusual seismicity. A data set of this size (nine events) is obviously not adequate to demonstrate specific effects but is large enough to suggest several interesting ones. As a general rule, each mechanism is subject to at least two possible interpretations!

We attempted to divide earthquakes into three groups based on location relative to the plate boundary: those in the overriding plate, those in the subducting plate, and those on the interface. To do this, the position of the interface must be identified, which is difficult to do from the low level of seismicity. Ideally, the interface can be identified from the location of large thrust earthquakes, a high level of seismicity, and phases reflected [Fukao et al., 1978] and converted [Snoke et al., 1977] at the slab surface. Without this information our assignments of earthquakes into groups is less certain.

The cross sections (Figure 3) suggest that for the depths discussed previously, the December 24, 1967, pair; the October 8, 1974; and May 29, 1978 events are within the upper plate. The November 13, 1966; March 19, 1953; and January 8, 1959, earthquakes appear to be within the downgoing plate. We believe that the May 15, 1969, event is actually on the interface; the March 10, 1976, event is close to the interface and may be within either plate or at the interface.

The absence of large thrust fault earthquakes during the period studied suggests that subduction in this arc is largely aseismic. The existence and recurrence of such earthquakes defines the proportion of seismic versus aseismic slip at the subduction zone [Kanamori, 1977]; only these earthquakes should be used in comparing slip rates from seismic moments to those obtained from relative plate motion calculations. Large intraplate events like the Christmas Day or October 8, 1974, normal fault earthquakes should not be used for this purpose. Similarly, their slip vectors have no direct relation to plate motion directions.

A discrepancy between the subduction rate predicted by plate motion models and that estimated from seismic moments has been noted by Molnar and Sykes [1969] and Westbrook [1975] using recent seismicity.

Similarly, Dorel [1981] used both recent and historical seismicity, with moments estimated from isoseismals, to estimate seismic slip rates and concluded that a substantial portion of aseismic slip is occurring. Such estimates provide an upper bound on the seismic slip, since the largest events in recent years are intraplate normal faults rather than interplate thrusts. It is difficult to say whether the large historic events of 1690 and 1843 [Dorel, 1981] were thrust events; the 1933 Sanriku and 1977 Indonesian earthquakes demonstrate that lithospheric normal faulting events can be extremely large. Thus despite the large uncertainties in the isoseismals-moment-slip rate estimates [Dorel, 1981], especially where the slip rate is so low, the conclusion of substantial aseismic slip seems plausible. Such aseismic slip is consistent with the observation of large normal faulting earthquakes seaward of the trench, assuming the Kanamori [1977] model. The alternative to aseismic decoupled subduction is, as always, the possibility that the sampling time is too short to record major intervals of seismic slip. The similarities between the instrumental and historic estimates argue against this possibility.

Intuitively, decoupling and aseismic slip seem highly plausible in an area where old lithosphere subducts slowly [Ruff and Kanamori, 1980]. Coupling is minimized by the slow convergence; the negative buoyancy force due to the weight of the slab is maximized and is then the dominant force in the arc system.

The overriding plate contains one of the two largest arc events, the October 8, 1974 Ms 7.4 Antigua earthquake, and three strike slip events. The Antigua event is quite interesting; like the other two magnitude seven events in the study, it is a normal fault, but in a very different location and orientation from the Christmas Day or March 19, 1953, earthquakes. Its mechanism shows NNW-SSE extension within the arc massif but well seaward of the Neogene volcanic arc.

The tectonic origin of this earthquake is unclear--normal faulting parallel to the arc is the more expected orientation and can be interpreted as grossly related to back arc extension and spreading. Normal faulting perpendicular to the arc has been observed for microearthquakes in the Adak region [LaForge and Engdahl, 1979] and interpreted as lateral extension of the overriding plate due to oblique subduction. This is one possible cause for the much larger October 8, 1974, earthquake [Dewey et al., 1980; McCann et al., 1982]. A second alternative is that strain is induced in the upper plate by lateral changes in the dip of the subduction zone. The explanation we prefer is a flexure of the overriding plate due to the subduction of the Barracuda Ridge shown in Figure 16 and discussed later. Faulting occurred at considerable depth within the overriding plate as indicated by the 40-km depth of the main shock; the aftershock zone indicates that a southeast dipping fault plane extends to a depth of 10 km [Dewey et al., 1980; McCann et al., 1982].

The three strike slip events in the upper plate could represent differential lateral block motion in response to the subduction. The P and T axes (Figure 15, top) show no particular consistency; the nodal planes and thus horizontal slip vector components are too variable to draw meaningful conclusions about the motion direction. Either the NW-SE planes, yielding strike slip motion grossly similar to the subduction direction, or the NE-SW planes, which align with a reentrant structure in the shallow platform of the arc, are perfectly plausible. These events are shallower than the large normal faulting earthquake. (Several other strike slip events given in the appendix were also shown by Dorel [1978].)

The May 15, 1969, thrust earthquake can be interpreted as slip on the subduction boundary. If so, the March 10, 1976, event is close to the boundary, may be in either plate, and as such is difficult to interpret tectonically beyond block faulting in one plate or the other.

Three events are clearly within the downgoing slab. Two are normal faults, one (November 13, 1966) near the slab surface and the other much larger (March 19, 1953) at a depth of 135 km. The third event (January 9, 1959) is almost pure strike slip at a similar depth of 141 km.

The Ms 7.5 March 19, 1953, earthquake suggests extension in the slab at depths below 100 km (Figure 16), in accord with suggestions that old lithosphere subducting slowly sinks freely under its own weight [Isacks and Molnar, 1969; Fujita and Kanamori, 1981]. The T axis does not appear to be in-plate, which would require a vertical rather than 45$^{\circ}$ dipping nodal plane. The stress field may be extensional but not exactly in-plate; alternatively, the faulting geometry may be controlled by a remanent fault formed in the early stages of subduction by a Christmas Day type normal fault earthquake. The true intraplate stress direction, as opposed to the T axis, would be in-plate.

The November 13, 1966, event occurs below the slab surface at a much shallower depth. It may result from in-plate compression due to the 'sagging' of the downgoing plate [Sleep, 1979] or 'unbending' [Engdahl and Scholz, 1977]. If so, this event could be the only manifestation of the stresses which at higher convergence rates and for younger lithosphere can produce double seismic zones; here they are almost completely overwhelmed by the extension due to the sinking slab [Fujita and Kanamori, 1981]. An alternate but not exclusive possibility is that slip occurs on a fracture remaining from a presubduction normal fault earthquake.

The last event at depth whose mechanism we studied shows almost pure strike slip and may represent tear faulting within the slab along an old fracture zone (Figure 16). The NW-SE plane is similar to the strike of the currently visible structures in the subducting plates and occurs at a site suggested by Tomblin [1975] and Dorel [1981] as an alignment of seismicity at depth, which can be seen in Figure 3 (sections DD' and GG'). (Contrast this cluster of seismicity to the location of the other large deep event, the March 19, 1953, normal fault, on sections EE' and GG'.) We interpret this as a possible fossil fracture zone; the buried aseismic ridge identified by Westbrook [1975] would intersect the arc farther south at Martinique. Tear faulting at depth along an old fracture zone has been identified in the New Hebrides by Chung and Kanamori [1978a].

This discussion leads to the questions of whether previously formed fractures will survive subduction as coherent features. The least disrupted feature would be one striking perpendicular to a trench where perpendicular subduction occurs. In many arcs, fracture zones will approximate this situation and should survive to considerable depths. Oblique subduction, or a strike not perpendicular to the trench, may produce some disruption of the fault. At the other extreme, faults parallel to the trench, such as those of earthquakes like the Christmas Day main shock may be disrupted seriously by the bending of the plate as it subducts. On the other hand, the faults may accommodate a portion of the bending through slip; the Chapple and Forsyth [1979] model for the formation of such faults interprets them as resulting from the bending stresses.

## Aseismic Ridge Subduction

Several aseismic ridges, most noticeably the Barracuda Ridge and the Tiburon Rise, intersect the subduction zone. The effects of aseismic ridge subduction have been discussed by many authors [Vogt et al., 1976; Kelleher and McCann, 1976; Chung and Kanamori, 1978a; Chung, 1979; McCann and Sykes, 1981; McCann et al., 1982]. Chung and Kanamori [1978a] noted a shallowing of seismicity and Benioff zone dip where the D'Entrecasteaux fracture zone subducts into the New Hebrides Trench. They also observed intermediate depth tear faulting along the flanks of the

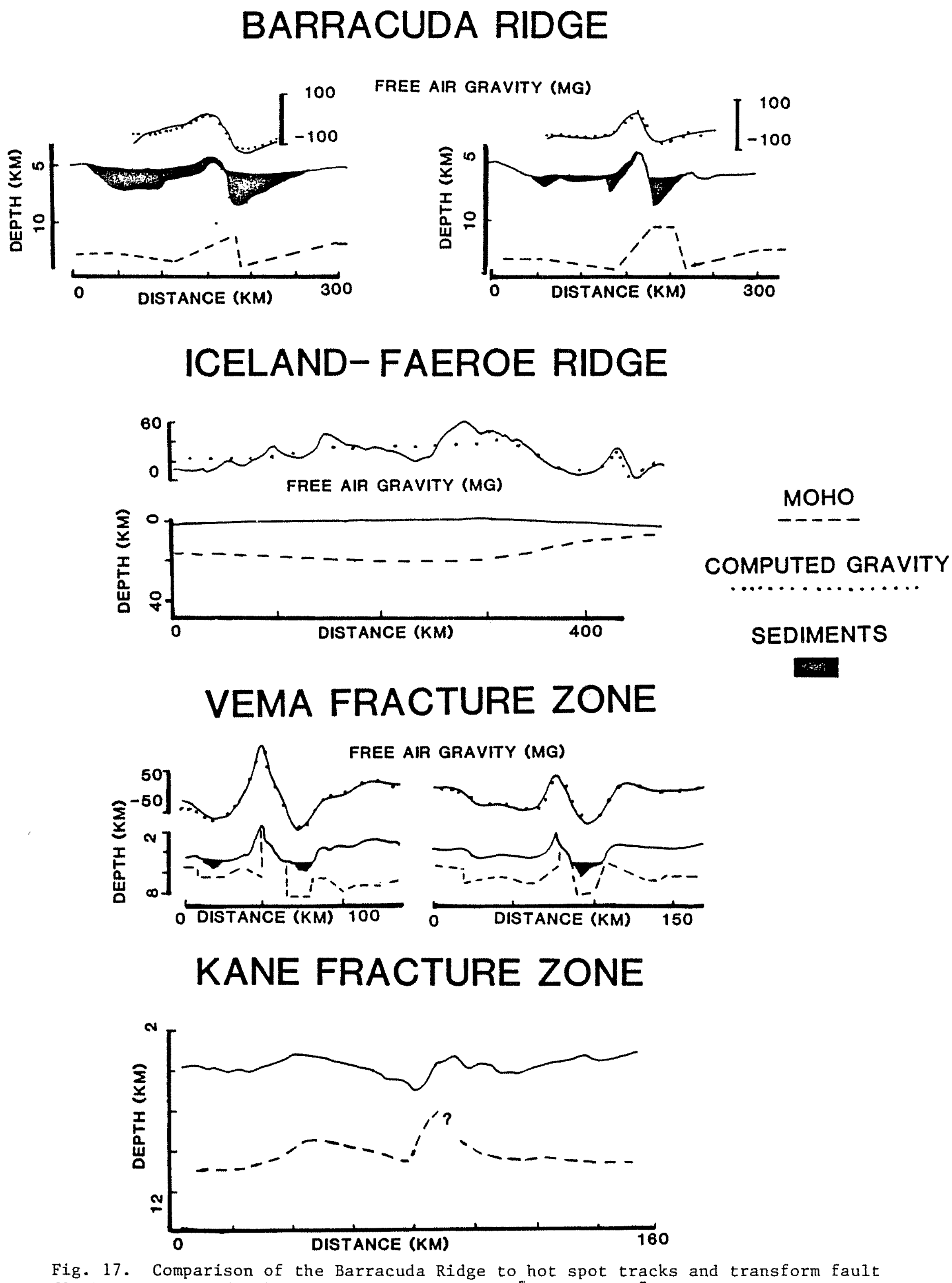


Fig. 17. Comparison of the Barracuda Ridge to hot spot tracks and transform fault flanking ridges. (top) Gravity data and model [Birch, 1970] showing crustal thinning. Sediment thickness was primarily controlled from seismic reflection. (Profile runs left to right, south to north.) (middle top) Gravity data and model [Bott et al., 1971] for a hot spot track, the Iceland-Faeroe Ridge, indicating crustal thickening. (middle bottom) Gravity data and model [Robb and Kane, 1975] for the Vema fracture zone and flanking ridge, indicating crustal thinning. (bottom) Seismic refraction results [Detrick and Purdy, 1980] for the Kane fracture zone and flanking ridge, showing crustal thinning.

aseismic ridge and interpreted these observations using a model of buoyant forces due to a subducting low-density ridge. Chung [1979] discussed several other locations using this model such as the Nazca Ridge; this area is also discussed by Pilger [1981].

The Lesser Antilles is a very different situation. In this case, the Barracuda Ridge does not seem to be buoyant. Figure 17 (top) shows a free air gravity profile across the Barracuda Ridge and a corresponding crustal model [Birch, 1970]. The inferred structure has a thin crust and shallow mantle. Due to this excess mass at depth a vertical section weighs more than the usual section of oceanic lithosphere, and such a ridge would not be buoyant. This structure is quite different from those inferred for many other aseismic ridges.

Figure 17 (second from top) shows a model of the Iceland-Faeroe Ridge [Bott et al., 1971]. This model is an Airy isostatic one, in which the ridge is compensated by a thicker crust at depth. The data can also be fit, less successfully, by a Pratt model. Crustal thickening has also been proposed for other aseismic ridges such as the Hawaiian-Emperor chain [Walcott, 1970; Watts and Cochran, 1974; Watts, 1978] and the Ninetyeast and Walvis ridges [Detrick and Watts, 1979]. All these features are now considered to be hot spot traces [Wilson, 1963; Morgan, 1972, 1981; Sclater and Fisher, 1974]; the mechanism of isostatic adjustment depends on the crustal properties at the time of ridge formation, but crustal thickening always occurs. Such ridges would thus be buoyant relative to usual oceanic lithosphere.

The Barracuda Ridge is clearly a different type of structure. A possible analogy might be the flanking ridge-transform pairs observed along several Atlantic fracture zones. These structures, which occur along the Vema [van Andel et al., 1971; Robb and Kane, 1975], Romanche [Cochran, 1973] and Kane [Detrick and Purdy, 1980] fracture zones, often have morphology similar to the Barracuda Ridge: a linear high with a parallel trough. The flanking ridges and fracture zones appear to be underlain by excess mass at shallow depth as indicated by gravity data. Figure 17 (third from top) shows Robb and Kane's [1975] model for the Vema fracture zone; the excess mass is produced by crustal thinning and a shallow Moho. Gravity models are nonunique; Cochran [1973] favored an anomalously high-density crust for the Romanche fracture zone. Refraction data for the Kane fracture zone [Detrick and Purdy, 1980] suggests that there the excess mass is due to thin crust and shallow mantle rather than high-density crust (Figure 17, bottom). The nature of the mass excess may not be the same for all flanking ridge and transform systems, but however distributed, it results in a negatively buoyant ridge.

The origin and nature of flanking ridges is unclear; Bonatti and Honnorez [1976] and Bonatti [1978] interpret them as dynamically uplifted blocks, which expose dense high-velocity upper mantle material. It is interesting that such structures are presently known primarily in the Atlantic and Indian oceans; if real, their absence in the Pacific may suggest that the formation is spreading rate dependent. It is possible that flanking ridge-fracture zone structures can survive away from the active transform segment and thus remain as ridges in old crust. Such ridges are quite different from the scarps produced at fracture zones by the thermal effects of the age contrast [Delong et al., 1977], which are isostatic and will subside with age unless locking occurs across the fracture zone [Sandwell and Schubert, 1981]. Age contrast scarps are always found along a fracture zone; flanking ridges occur only in a few places.

The crucial point is that not all aseismic ridges (topographic highs might be a better phrase) can be considered buoyant upon subduction. Hot spot traces like the Nazca Ridge should be buoyant; transform flanking ridges are the opposite. Essentially, features compensated at depth with thick crust should be buoyant; those underlain by dense material and supported by crustal rigidity should have negative buoyancy. Determination if a feature is buoyant must be made on a case-by-case basis, especially since a ridge associated with a fracture zone can be either a fossil flanking ridge, a hot spot trace (Ninetyeast, Chagos), or a pure age difference effect.

Both buoyant and nonbuoyant topographic highs can have major effects on the subduction process. A nonbuoyant feature, such as the Barracuda Ridge, can flex the overriding plate solely because of its elevation (perhaps as shown by the October 8, 1974, normal event), or interact mechanically with the upper plate in some other fashion (for example, if the tip of the ridge is in contact with the upper plate). On the other hand, a nonbuoyant feature should not cause shallowing of the subduction zone dip. The tear faulting along an aseismic ridge [Chung and Kanamori, 1978a] could occur for either buoyant or nonbuoyant ridges--the vertical motion component would be opposite. Another possible difference between transform flanking ridges and hot spot tracks is that while the latter is continuous, the former may be formed only under isolated (not yet understood) conditions and thus may be discontinuous. If a hot spot track ridge is observed at a trench, it generally continues on the downgoing plate; a flanking ridge which enters the trench may or may not continue the full length of the subducting slab.

## Plate Motions

The focal mechanism data along the arc show no clear evidence for a North America-South America-Caribbean triple junction. In particular, the only strike slip faulting in the subducting plate near the trench seems to be in aftershocks of the December 25, 1969, normal faulting event.

The seismicity level and possible Benioff zone dip changes along the arc are real and unexplained; Vierbuchen's [1979] suggestion that the seismicity change is related to the NA-SA boundary is plausible but not confirmable by this study. We did observe strike slip faulting at depth in the region proposed by Vierbuchen [1979] as the boundary, which corresponds to an active seismic trend cutting the subduction zone. Whether this is a fossil fracture or a current boundary is hard to say; shallow strike slip faulting, especially near the trench, would be more convincing evidence for a boundary.

The alternative to a discrete boundary is a wide zone of distributed motion. Possibly the Atlantic 'intraplate' events reflect such a zone; all three have some strike slip component with a similar sense of motion. Left-lateral motion on the NE-SW steeply dipping planes would fit model RM1 [Minster et al., 1974; Jordan, 1975] (Figure 2) both in direction and in sense of motion. The alternative, right lateral on the shallow dipping NW-SE planes, seems less appealing but would fit the newer RM2 [Minster and Jordan, 1978]. The 1964 and 1977-78 events cannot lie on a single transform boundary, and thus any attempt to relate them to a boundary must involve a diffuse zone. It is also difficult to tie these events to the deep strike slip event near Dominica; the sense of strike slip is not consistent on the NE-SW plane. The Atlantic events and the Dominica event can only be consistent if the boundary turns to have a NW-SE trend at depth in the arc, parallel to the westmost portions of the Barracuda Ridge and Tiburon Rise. In this case the boundary could not be a single small circle and would have to be part of a complex diffuse zone.

This level of seismicity (two of the events are respectably sized intraplate earthquakes) is a noticeable feature and perhaps what might be expected for such a slow motion boundary. Alternatively, some of this motion might be aseismic. The lack of bathymetric expression (for example, no clear offset across the Barracuda Ridge) for such a boundary may be due to its slow nature. Furthermore, since any NA-SA motion results from small differences in NA-AF and SA-AF motion, it is not clear that the sense of motion has been constant with time; perhaps reversals in the motion have reduced any observable offset on many bathymetric structures. Nonetheless, the few Atlantic events can also be regarded as N-S intraplate compression [Bergman and Solomon, 1980].

## Conclusions

Several basic conclusions can be drawn from the data presented for the Lesser Antilles. The results have implications for other arcs and the subduction process in general.

1. During the time period studied, subduction is largely decoupled and aseismic. Most seismicity is intraplate and only a small fraction of the slip occurs as interface thrust earthquakes.
2. Large normal faulting earthquakes occur in the subducting plate seaward of the trench. The aftershocks of such an earthquake show both continued normal faulting and strike slip on planes quite different from the normal fault, presumably weak zones in the oceanic lithosphere.
3. The downgoing slab is in a state of extension. Some faulting may occur by reactivation of presubduction structures (fracture zones) or structures formed during the early stages of subduction (normal faults).
4. The subduction of bathymetric highs may affect the seismicity of the overriding plate; in particular, an unusually oriented large normal event may be a consequence. The Barracuda Ridge is not buoyant and thus cannot effect the overall dip of the Benioff zone.
5. There is no direct evidence for a North America-South America boundary in the focal mechanism data; though several pieces of data are consistent with such a boundary, any possible correlations between seismicity changes along the arc and the hypothesized boundary are not provable.

TABLE A1. Focal Mechanisms for the Lesser Antilles and Northeast Venezuela

| Number | Date | Lat. °N | Lon. °W | Depth | m | Ms | Reference |
|---|---|---|---|---|---|---|---|
| 1 | September 7, 1974 | 15.10 | 60.63 | 53 | 5.7 | | D |
| 2 | January 8, 1959 | 15.25 | 61.26 | 140 | | 6.5 | S |
| 3 | March 22, 1973 | 15.34 | 61.29 | 151 | 5.0 | | D |
| 4 | May 15, 1969 | 16.75 | 61.39 | 50 | 5.7 | 6.0 | D |
| 5 | July 15, 1966 | 16.99 | 61.49 | 62 | 5.3 | | D |
| 6 | November 13, 1966 | 17.05 | 61.94 | 73 | 5.4 | | S,D |
| 7 | October 8, 1974 | 17.37 | 61.99 | 41 | 6.6 | 7.4 | S,R,D,W |
| 8 | May 31, 1960 | 17.72 | 61.63 | 27 | | 6.0 | M |
| 9 | May 29, 1978 | 17.21 | 61.59 | 25 | 5.2 | 5.4 | S |
| 10 | December 24, 1967 (2003) | 17.42 | 61.19 | 15 | 6.1 | 6.3 | S,R,D |
| 11 | December 24, 1967 (2132) | 17.61 | 61.26 | 17 | 5.9 | | S,D |
| 12 | October 14, 1967 | 17.33 | 60.89 | 42 | 5.3 | | D |
| 13 | March 10, 1976 | 16.84 | 61.06 | 56 | 5.7 | 6.2 | S |
| 14 | December 1, 1969 | 16.68 | 60.80 | 47 | 5.5 | | D |
| 15 | December 25, 1969 (2231) | 16.08 | 59.79 | 47 | 5.8 | | S,D |
| 16 | October 23, 1964 | 19.80 | 56.11 | 30 | 6.2 | 6.8 | S,L,M |
| 17 | December 29, 1969 | 16.18 | 59.74 | 27 | 5.5 | 5.9 | S,D |
| 18 | December 6, 1978 | 17.44 | 54.83 | 10 | 5.4 | | S |
| 19 | January 7, 1970 | 15.86 | 59.79 | 40 | 5.5 | 6.2 | S,D |
| 20 | December 13, 1977 | 17.33 | 54.91 | 25 | 5.7 | 6.9 | S,B |
| 21 | December 25, 1969 (2132) | 15.79 | 59.64 | 42 | 6.4 | 7.5 | S,R,D |
| 22 | December 26, 1969 | 15.79 | 59.56 | 35 | 5.2 | | S,D |
| 23 | March 19, 1968 | 14.06 | 60.47 | 57 | 5.0 | | D |
| 24 | August 20, 1964 | 10.87 | 60.49 | 79 | 5.4 | | M,D |
| 25 | January 4, 1967 | 10.70 | 62.50 | 74 | 6.4 | | M |

TABLE A1. (Continued)

| Number | Date | Lat. °N | Lon. °W | Depth | m | Ms | Reference |
|---|---|---|---|---|---|---|---|
| 26 | July 14, 1963 | 10.45 | 62.73 | 20 | 5.8 | | M |
| 27 | August 10, 1964 | 9.15 | 62.02 | 51 | 5.4 | | V |
| 28 | May 14, 1966 | 10.38 | 63.05 | 37 | 5.4 | | M |
| 29 | July, 1979 (composite) | 10.45 | 63.17 | <10 | | | P |
| 30 | July, 1979 (composite) | 10.50 | 63.25 | <15 | | | P |
| 31 | June, 1979 (composite) | 10.40 | 63.60 | <15 | | 6.5 | P |
| 32 | June, 1979 (composite) | 10.45 | 63.60 | <5 | | 6.1 | P |
| 33 | July 12, 1974 | 10.64 | 63.47 | 34 | 6.2 | | R,V |
| 34 | October 2, 1957 | 10.94 | 62.80 | 60 | | | M |
| 34 | September 20, 1968 | 10.76 | 62.70 | 103 | | | T,V |

B, Bergman and Solomon [1980]; D, Dorel [1978]; L, Liu and Kanamori [1980]; M, Molnar and Sykes [1969]; P, Perez and Aggarwal [1981]; R, Rial [1978]; S, this study; T, Tomblin [1975]; V, Vierbuchen [1979]; W, Dewey et al. [1980] and McCann et al. [1982].

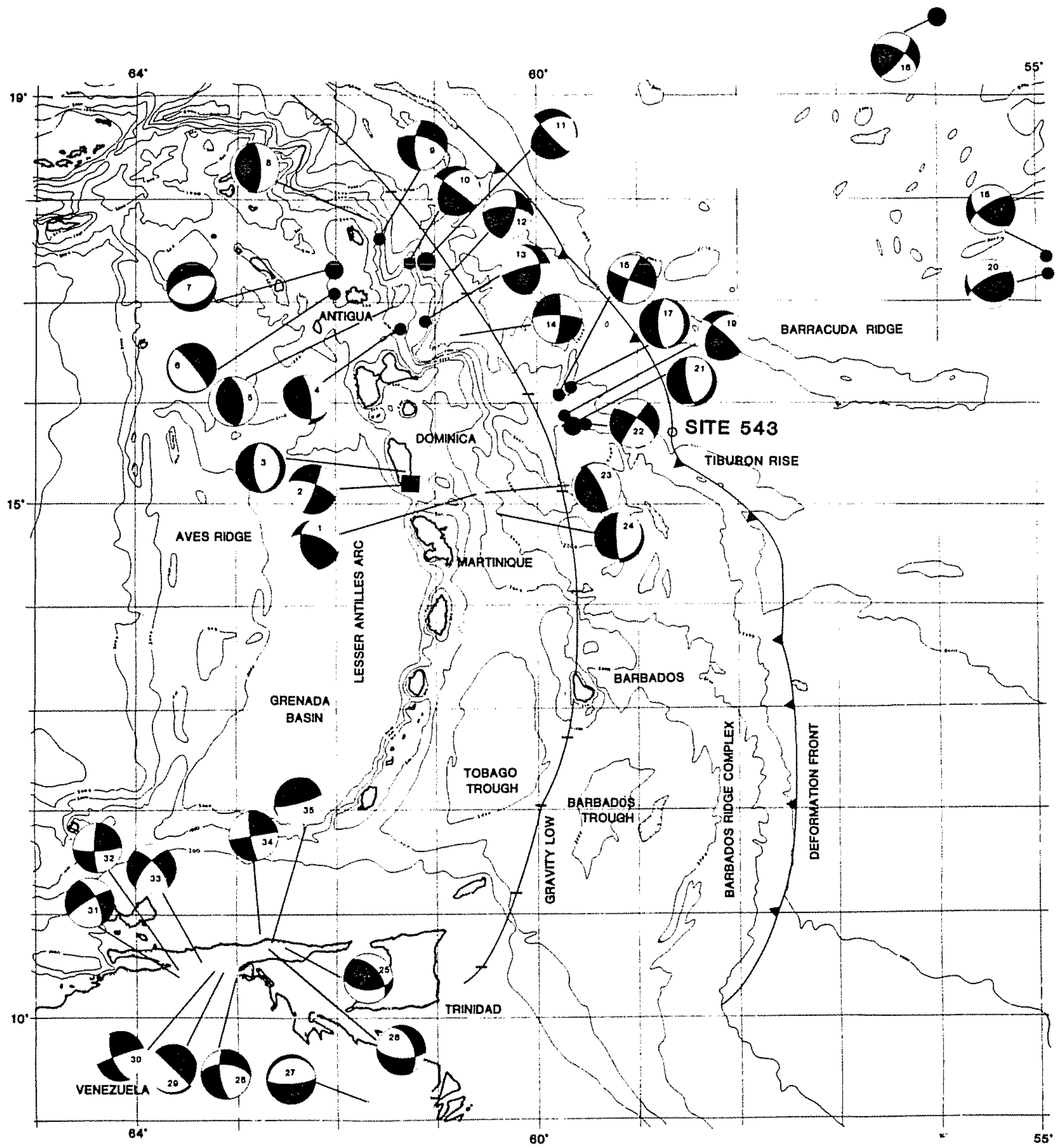


Fig. A1. Focal mechanism results from this and previous studies corresponding to the list in the appendix. Dots or squares (same conventions as Figure 1) indicate results of this study.

Acknowledgments. We have benefited from discussions with and assistance from colleagues in the Barbados Regional Synthesis Group: Bernard Biju-Duval, John Ladd, Casey Moore, John Saunders, Jane Schoonmaker, Jean-Francois Stephan, and Graham Westbrook. We also thank Carl Bowin, Kevin Burke, Wai-Ying Chung, Richard Gordon, Jim Dewey, Jason Morgan, Frank Richter, Tetsuzo Seno, and Norman Sleep for valuable discussions; Glenn Kroeger for the use of his body wave modeling routines; Jacques Dorel and John Tomblin for their results prior to publication; and Craig Bina and April Poelvoorde for technical assistance. This research was supported by Joint Oceanographic Institutions, Inc., NSF grant EAR 8007363, a Cottrell Research Grant, and a Petroleum Research Fund (American Chemical Society) grant at Northwestern and NSF grant EAR 8025267 at Michigan State.

## References

Abe, K., Lithospheric normal faulting beneath the Aleutian trench, Phys. Earth Planet. Inter., 5, 190-198, 1972.

Ball, M. M., and C. G. Harrison, Crustal plates in the central Atlantic, Science, 167, 1128-1129, 1970.

Bergman, E. A., and S. C. Solomon, Intraplate earthquakes: Implications for local and regional intraplate stress, J. Geophys. Res., 85, 5389-5410, 1980.

Biju-Duval, B., A. Mascle, L. Montadert, and J. Wanneson, Seismic investigations in the Columbia, Venezuela and Grenada Basins, and on the Barbados Ridge for future IPOD drilling, Geol. Mijnbouw, 57, 105-116, 1978.

Birch, F. S., The Barracuda Fault Zone in the western North Atlantic: Geological and geophysical studies, Deep Sea Res., 17, 847-859, 1970.

Bonatti, E., Vertical tectonism in oceanic fracture zones, Earth Planet. Sci. Lett., 37, 369-379, 1978.

Bonatti, E., and J. Honnorez, Sections of the earth's crust in the equatorial Atlantic, J. Geophys. Res., 81, 4104-4116, 1976.

Bott, M., C. Browitt, and A. Stacey, The deep structure of the Iceland-Faeroe Ridge, Mar. Geophys. Res., 1, 328-351, 1971.

Bowin, C., Caribbean gravity field and plate tectonics, Spec. Pap., Geol. Soc. Am., 169, 1976.

Boynton, C., G. Westbrook, M. Bott, and R. Long, A seismic refraction investigation of crustal structure beneath the Lesser Antilles arc, Geophys. J. R. Astron. Soc., 58, 371-394, 1979.

Burke, K., P. J. Fox, and A. M. C. Sengor, Buoyant ocean floor and the evolution of the Caribbean, J. Geophys. Res., 83, 3949-3945, 1978.

Burke, K., J. Grippi, and A. M. C. Sengor, Neogene structures in Jamaica and the tectonic style of the Northern Caribbean plate boundary zone, J. Geol., 88, 375-386, 1980.

Bunce, E. T., J. D. Phillips, R. L. Chase, and C. O. Bowin, The Lesser Antilles arc and the eastern margin of the Caribbean Sea, Sea, vol. 4, 359-386, 1970.

Cardwell, R., E. Kappel, M. Lawrence, and B. Isacks, Plate convergence along the Indonesian Arc (abstract), Eos Trans. AGU, 62, 404, 1981.

Case, J. E., and T. L. Holcombe, Geologic-tectonic map of the Caribbean region, U.S. Geol. Surv. Misc. Invest. Map, I-1100, 1980.

Chapple, W. M., and D. W. Forsyth, Earthquakes and the bending of plates at trenches, J. Geophys. Res., 84, 6729-6749, 1979.

Chase, C. G., Plate kinematics: The Americas, East Africa, and the rest of the world, Earth Planet. Sci. Lett., 37, 355-368, 1978.

Chase, R. L., and E. T. Bunce, Underthrusting of the eastern margin of the Antilles by the floor of the western North Atlantic Ocean and the origin of the Barbados Ridge, J. Geophys. Res., 74, 1413-1420, 1969.

Chen, A. T., C. Frolich, and G. V. Latham, Seismicity of forearc marginal wedges (accretionary prisms), J. Geophys. Res., 87, 3679-3690, 1982.

Chen, T., and D. Forsyth, A detailed study of two earthquakes seaward of the Tonga trench: Implications of mechanical behavior of the oceanic lithosphere, J. Geophys. Res., 83, 4495-5004, 1978.

Chung, W.-Y., A seismological investigation of the subduction mechanism of aseismic ridges, part II, Ph.D. thesis, Calif. Inst. of Technol., Pasadena, 1979.

Claerbout, J. F., Fundamentals of Geophysical Data Processing, McGraw-Hill, New York, 1976.

Cochran, J., Gravity and magnetic investigations of the Guiana basin, western equatorial Atlantic, Geol. Soc. Am. Bull., 84, 3249-3268, 1973.

Davies, G. F., Mechanics of subducted lithosphere, J. Geophys. Res., 85, 6304-6318, 1980.

Delong, S., J. Dewey, and P. Fox, Displacement history of oceanic fracture zones, Geology, 5, 199-202, 1977.

Detrick, R., and G. Purdy, The crustal structure of the Kane fracture zone from seismic refraction studies, J. Geophys. Res., 85, 3759-3777, 1980.

Detrick, R., and A. Watts, An analysis of isostasy in the world's oceans, 3, Aseismic ridges, J. Geophys. Res., 84, 3637-3653, 1979.

Dewey, J. W., W. R. McCann, A. J. Murphy, and S. T. Harding, A large normal fault earthquake in the overriding wedge of the Antilles subduction zone; the Antigua earthquake of October 8, 1974 (abstract), Eos Trans. AGU, 61, 295, 1980.

Dorel, J., Sismicite et structure de l'arc des Petites Antilles et du Bassin Atlantique, these de doctorat, Univ., Pierre et Marie Curie, Paris, 1978.

Dorel, J., Seismicity and seismic gaps in the Lesser Antilles arc and earthquake hazards in Guadeloupe, Geophys. J. R. Astron. Soc., 67, 679-696, 1981.

Engdahl, E., and C. Scholz, A double Benioff zone beneath the central Aleutians: An unbending of the lithosphere, Geophys. Res. Lett., 4, 473-476, 1977.

Fitch, T. J., R. G. North, and M. W. Shields, Focal depths and moment tensor representations of shallow earthquakes associated with the great Sumba earthquake, J. Geophys. Res., 86, 9357-9374, 1981.

Forsyth, D. W., Determinations of focal depths of earthquakes associated with the bending of oceanic plates at trenches, Phys. Earth. Planet. Inter., 28, 141-160, 1982.

Fujita, K., and H. Kanamori, Double seismic zones and stresses of intermediate depth earthquakes, Geophys. J. R. Astron. Soc., 66, 131-156, 1981.

Fujita, K., E. R. Engdahl, and N. H. Sleep, Subduction zone calibration and teleseismic relocation of thrust zone events in the central Aleutian Islands, Bull. Seismol. Soc. Am., 71, 1805-1828, 1981.

Fukao, Y., K. Kango, and I. Nakamura, Deep seismic zone as an upper mantle reflector of body waves, Nature, 272, 606-608, 1978.

Geller, R. J., Scaling relations for earthquake source parameters and magnitudes, Bull. Seismol. Soc. Am., 66, 1501, 1523, 1976.

Hasegawa, A., N. Umino, and A. Takagi, Double-planed structure of the deep seismic zone in the northeastern Japan arc, Tectonphysics, 47, 43-58, 1978.

Holcombe, T., P. Vogt, J. Matthews, and R. Murchison, Evidence for seafloor spreading in the Cayman Trough, Earth Planet. Sci. Lett., 20, 357-371, 1973.

Hong, T. L., and K. Fujita, Modelling of depth phases and source processes of some central Aleutian earthquakes, Earth Planet. Sci. Lett., 53, 333-342, 1981.

Helmberger, D. V., and L. J. Burdick, Synthetic seismograms, Annu. Rev. Earth Planet. Sci., 7, 417-442, 1979.

Isacks, B., and P. Molnar, Mantle earthquake mechanisms and the sinking of the lithosphere, Nature, 223, 1121-1124, 1969.

Jordan, T. H., The present-day motions of the Caribbean plate, J. Geophys. Res., 80, 4433-4439, 1975.

Kanamori, H., Velocity and Q of mantle waves, Phys. Earth Planet. Inter., 2, 259-275, 1970.

Kanamori, H., Seismological evidence of a lithospheric normal faulting--The Sanriku earthquake of 1933, Phys. Earth Planet. Inter., 4, 289-300, 1971.

Kanamori, H., Seismic and aseismic slip along subduction zones and their tectonic implications, in Island Arcs, Deep Sea Trenches and Back-Arc Basins, Maurice Ewing Ser., vol. 1, edited by M. Talwani and W. C. Pitman III, pp. 162-174, AGU, Washington, D.C., 1977.

Kanamori, H., and D. L. Anderson, Theoretical basis of some empirical relations in seismology, Bull. Seismol. Soc. Am., 65, 1073-1095, 1975.

Kanamori, H., and G. S. Stewart, Mode of strain release along the Gibbs fracture zone, Mid-Atlantic Ridge, Phys. Earth Planet. Inter., 11, 312-332, 1976.

Keary, P., G. Peter, and G. Westbrook, Geophysical maps of the eastern Caribbean, J. Geol. Soc. London, 131, 311-321, 1975.

Kelleher, J., and W. McCann, Buoyant zones, great earthquakes, and unstable boundaries of subduction, J. Geophys. Res., 81, 4885-4896, 1976.

Ladd, J., Relative motion of South America with respect to North America and Caribbean tectonics, Geol. Soc. Am. Bull., 87, 969-976, 1976.

LaForge, R., and E. Engdahl, Tectonic implications of seismicity in the Adak Canyon region, Central Aleutians, Bull. Seismol. Soc. Am., 69, 1515-1532, 1979.

Langston, C. A., and D. V. Helmberger, A procedure for modelling shallow dislocation sources, Geophys. J. R. Astron. Soc., 42, 117-130, 1975.

Le Douaran, S., and J. Francheteau, Axial depth anomalies from $10^{\circ}$ to $50^{\circ}$ north along the Mid-Atlantic Ridge: Correlation with other mantle properties, Earth Planet. Sci. Lett., 54, 29-47, 1981.

Liu, H.-L., and H. Kanamori, Determination of source parameters of midplate earthquakes from the wave forms of body waves, Bull. Seismol. Soc. Am., 70, 1989-2004, 1980.

Macdonald, K., and T. Holcombe, Inversion of magnetic anomalies and seafloor spreading in the Cayman Trough, Earth Planet. Sci. Lett., 40, 407-414, 1978.

Mascle, A., D. Lajat, and G. Nely, Sediment deformation linked to subduction and to argillokinesis in the southern Barbados Ridge from multichannel seismic surveys, in Transactions of the Fourth Latin American Geological Congress, in press, 1981.

McCann, W. R., and L. R. Sykes, Subduction of aseismic ridges in the northeastern Caribbean: Effects on seismicity and arc morphology (abstract), Eos Trans. AGU, 62, 323, 1981.

McCann, R. W., J. W. Dewey, A. J. Murphy, and S. T. Harding, A large normal fault earthquake in the ovveriding wedge of the Lesser Antilles subduction zone: The earthquake of October 8, 1974, Bull. Seismol. Soc. Am., in press, 1982.

McKenzie, D. P., The relation between fault plane solutions for earthquakes and the directions of the principal stresses, Bull. Seismol. Soc. Am., 59, 591-601, 1969.

Minster, J. B., and T. H. Jordan, Present-day plate motions, J. Geophys. Res., 83, 5331-5354, 1978.

Minster, J. B., T. H. Jordan, P. Molnar, and E. Haines, Numerical modelling of instantaneous plate tectonics, Geophys. J. R. Astron. Soc., 36, 541-576, 1974.

Molnar, P., and L. R. Sykes, Tectonics of the Caribbean and middle America regions from focal mechanisms and seismicity, Geol. Soc. Am. Bull., 80, 1639-1684, 1969.

Molnar, P., D. Freedman, and J. S. F. Shih, Length of intermediate and deep seismic zones and temperatures in downgoing slabs of lithosphere, Geophys. J. R. Astron. Soc., 56, 41-54, 1979.

Moore, J. C., B. Biju-Duval, J. A. Bergen, G. Blackinton, G. E. Claypool, D. S. Cowan, F. Duennebier, R. T. Guerro, C. J. Hemleben, D. Hussong, M. S. Marlow, J. H. Natland, C. J. Pudsey, G. W. Renz, M. Tardy, M. E. Wissis, D. Wilson, and A. Wright, Offscraping and underthrusting of sediment at the deformation front of the Barbados Ridge: Results from leg 78 DSDP, submitted to Geol. Soc. Am. Bull., 1981.

Morgan, W. J., Deep mantle convection plumes and plate motions, Am. Assoc. Pet. Geol. Bull., 56, 203-213, 1972.

Morgan, W. J., Hotspot tracks and the opening of the Atlantic and Indian oceans, Sea, 7, 443-487, 1981.

Perez, O. J., and Y. P. Aggarwal, Present-day tectonics of southeastern Caribbean and northeastern Venezuela, J. Geophys. Res., 86, 10791-10805, 1981.

Peter, G., and G. K. Westbrook, Tectonics of southwestern north Atlantic and Barbados Ridge complex, Am. Assoc. Pet. Geol. Bull., 60, 1078-1106, 1976.

Pilger, R. H., Plate reconstructions, aseismic ridges and low angle subduction beneath the Andes, Geol. Soc. Am. Bull., 92, 448-456, 1981.

Rial, J., Seismic wave transmission across the Caribbean plate: High attenuation of the concave side of the Lesser Antilles arc, Bull. Seismol. Soc. Am., 66, 1905-1920, 1976.

Rial, J. A., The Caracas, Venezuela earthquake of July 1967: A multiple-source event, J. Geophys. Res., 83, 5405-5414, 1978.

Robb, J., and M. Kane, Structure of the Vema fracture zone from gravity and magnetic profiles, J. Geophys. Res., 80, 4441-4445, 1975.

Ruff, L., and H. Kanamori, Seismicity and the subduction process, Phys. Earth Planet. Inter., 23, 240-252, 1980.

Sandwell, D. T., and G. Schubert, Lithospheric stresses from geoid profiles across fracture zones (abstract), Eos Trans. AGU, 62, 390, 1981,

Sclater, J. G., and R. L. Fisher, The evolution of the east central Indian Ocean, with emphasis on the tectonic setting of the Ninetyeast Ridge, Geol. Soc. Am. Bull., 85, 683-702, 1974.

Seno, T., and B. Pongsawat, A triple-planed structure of seismicity and earthquake mechanisms at the subduction zone off Miyagi prefecture, northern Honshu, Japan, Earth Planet. Sci. Lett., 55, 25-36, 1981.

Sleep, N., Teleseismic P-wave transmission through slabs, Bull. Seismol. Soc. Am., 63, 1349-1373, 1973.

Sleep, N., The double seismic zone in downgoing slabs and the viscosity of the mesosphere, J. Geophys. Res., 84, 4565-4571, 1979.

Snoke, J., I. Sacks, and H. Okada, Determination of subducting lithosphere boundary by use of converted phases, Bull. Seismol. Soc. Am., 67, 1051-1060, 1977.

Speed, R. C., New views on the geology of Barbados, in Transactions of the Fourth Latin American Geological Congress, in press, Trinidad, 1981a.

Speed, R. C., Geology of Barbados: Implications for an accretionary origin, Oceanol. Acta, in Proceedings of the International Geological Congress, Paris, pp. 259-265, 1981b.

Starr, A., Slip in a crystal and rupture in a solid due to shear, Proc. Cambridge Philos. Soc., 24, 489-500, 1928.

Stauder, W., Mechanism of the Rat Island Earthquake sequence of February 4, 1965, with relation to island arcs and seafloor spreading, J. Geophys. Res., 73, 3847-3858, 1968.

Stein, S., An earthquake swarm on the Chagos-laccadive Ridge and its tectonic implications, Geophys. J. R. Astron. Soc., 55, 577-588, 1978.

Stein, S., Intraplate seismicity on bathymetric features: The 1968 Emperor Trough earthquake, J. Geophys. Res., 84, 4763-4768, 1979.

Stein, S., and G. Kroeger, Estimating earthquake source parameters from seismological data, in Solid Earth Geophysics and Geotechnology, edited by S. Nemet-Nassar, American Society of Mechanical Engineers, New York, 1980.

Stewart, G. S., Implications for plate tectonics of the August 19, 1977, Indonesian decoupling normal fault earthquake (abstract), Eos Trans. AGU, 59, 326, 1978.

Sykes, L. R., and M. Ewing, The seismicity of the Caribbean region, J. Geophys. Res., 70, 5065-5074, 1965.

Tomblin, J. F., The Lesser Antilles and Aves Ridge, in The Ocean Basins and Margins, vol. 3, edited by A. Nairn and F. Stehli, pp. 1-64, Plenum, New York, 1975.

Tsai, Y. B., and K. Aki, Simultaneous determination of the seismic moment and attenuation of seismic surface waves, Bull. Seismol. Soc. Am., 59, 275-287, 1969.

Uyeda, S., and H. Kanamori, Back arc opening and the mode of subduction, J. Geophys. Res., 84, 1049-1061, 1979.

van Andel, T., R. Von Herzen, and J. Phillips, The Vema fracture zone and the tectonics of transverse shear zones in oceanic crustal plates, Mar. Geophys. Res., 1, 261-283, 1971.

Vierbuchen, R. C., Jr., The tectonics of northeastern Venezuela and the southeastern Caribbean Sea, Ph.D. thesis, 193 pp., Princeton Univ., Princeton, N.J., 1979.

Vogt, P. R., A. Lowrie, D. R. Bracey, and R. N. Hey, Subduction of aseismic oceanic ridges: Effects on shape seismicity and other characteristics of consuming plate boundaries, Spec. Pap. Geol. Soc. Am., 172, 1976.

Walcott, R., Flexure of the lithosphere at Hawaii, Tectonophysics, 9, 435-446, 1970.

Watts, A., An analysis of isostasy in the world's oceans, 1, Hawaiian-Emperor seamount chain, J. Geophys. Res., 83, 5989-6004, 1978.

Watts, A., and J. Chchran, Gravity anomalies and flexure of the lithosphere along the Hawaiian-Emperor seamount chain, Geophys. J. R. Astron. Soc., 38, 119-141, 1974.

Westbrook, G. K., The structure of the crust and upper mantle in the region of Barbados and the Lesser Antilles, Geophys. J. R. Astron. Soc., 43, 201-242, 1975.

Westbrook, G., The Barbados Ridge Complex: Tectonics of a mature forearc system, Trench and Forearc Sedimentation and Tectonics, edited by J. K. Legett, in press, Blackwells, London, 1981.

Wilson, J., Evidence from islands on the spreading of the ocean floors, Nature, 197, 536-538, 1963.

(Received October 1, 1981;
revised May 14, 1982;
accepted May 21, 1982.)